

SMC++: Masked Learning of Unsupervised Video Semantic Compression

Yuan Tian, Guo Lu, and Guangtao Zhai

Abstract—Most video compression methods focus on human visual perception, neglecting semantic preservation. This leads to severe semantic loss during the compression, hampering downstream video analysis tasks. In this paper, we propose a Masked Video Modeling (MVM)-powered compression framework that particularly preserves video semantics, by jointly mining and compressing the semantics in a self-supervised manner. While MVM is proficient at learning generalizable semantics through the masked patch prediction task, it may also encode non-semantic information like trivial textural details, wasting bitcost and bringing semantic noises. To suppress this, we explicitly regularize the non-semantic entropy of the compressed video in the MVM token space. The proposed framework is instantiated as a simple Semantic-Mining-then-Compression (SMC) model. Furthermore, we extend SMC as an advanced SMC++ model from several aspects. First, we equip it with a masked motion prediction objective, leading to better temporal semantic learning ability. Second, we introduce a Transformer-based compression module, to improve the semantic compression efficacy. Considering that directly mining the complex redundancy among heterogeneous features in different coding stages is non-trivial, we introduce a compact blueprint semantic representation to align these features into a similar form, fully unleashing the power of the Transformer-based compression module. Extensive results demonstrate the proposed SMC and SMC++ models show remarkable superiority over previous traditional, learnable, and perceptual quality-oriented video codecs, on three video analysis tasks and seven datasets. *Codes and model are available at: <https://github.com/tianyuan168326/VideoSemanticCompression-Pytorch>.*

Index Terms—Video Compression, Masked Image/Video Modeling, Video Action Recognition.

1 INTRODUCTION

VIDEO compression has been researched over the past few decades. Most methods, including traditional [1] [2] and learnable ones [3] [4], aim at accurately reconstructing the video pixels, rather than preserving semantic information such as object shapes. These methods usually perform unfavorably on downstream AI tasks [5] [6].

To tackle this problem, lots of research efforts have been devoted to emphasizing the coding of semantics-relevant information. For example, early works [7] [8] [9] and standards [10] [11] [12] additionally transport the manually-designed image descriptors. Later, some methods [13] [14] [15] improve the traditional codec with hand-crafted designs to better cope with the specific tasks. Meanwhile, some methods [16] [17] [18] [19] [20] [21] compress the feature maps of AI models instead of the images, where the downstream task modules shall be fine-tuned to accommodate the features. Besides, scalable coding methods [22] [23] [24] [25] [26] [27] [28] divide the bitstream into two parts, *i.e.*, one for analysis tasks and another one for video reconstruction. The former part is usually optimized by task-specific losses.

Despite these progresses, rare methods are unsupervised and also support out-of-the-box deployment. *Unsupervised* represents that the semantic learning procedure is supervised by the video itself, without leveraging any human-annotated task labels. This is friendly to data scarcity scenarios and eliminates the labor of video annotation. *Out-of-*

the-box denotes the compressed videos can be directly consumed by the pre-trained downstream task models, without adapting or fine-tuning these numerous task models. This reduces the deployment cost and improves the practicality.

We refer to this novel and challenging problem as Unsupervised Video Semantic Compression (UVSC). Similar to traditional video compression [29], UVSC also pursues better video quality at the given bitrate. But, the main discrepancy lies in the quality metric. Traditional video compression focuses on low-level metrics like PSNR or SSIM [30]. Conversely, UVSC prefers a good semantic quality, which is an open challenge, since the high-level semantics is not well-defined like low-level information.

In this paper, motivated by the superior semantic learning capability of the masked video modeling (MVM) [31] [32] scheme, we propose the first MVM-powered video semantic compression framework. During the optimization, we mask out a large proportion of the compressed video patches, and use the unmasked parts to predict the masked regions, facilitating the compressed video patches by our framework to maintain their semantic attributes. Further, we notice that, while the MVM scheme is powerful in learning semantics, its inner generative learning paradigm also facilitates the coding framework memorizing non-semantic information [33], which makes the learned semantic feature consuming extra bitcost, as well as noisy.

To suppress this deficiency, we explicitly decrease the non-semantic information entropy of the MVM feature space, by formulating it as a parameterized Gaussian Mixture Model conditioned on the mined video semantics. The alternative semantic learning and non-semantic suppressing procedures make the system bootstrapping itself toward more efficient semantic coding. As a result, it shows remark-

- Yuan Tian is with the Shanghai AI Laboratory, Shanghai, China. E-mail: tianyuan@pjlab.org.cn.
- Guo Lu and Guangtao Zhai are with the Institute of Image Communication and Network Engineering, Shanghai Jiao Tong University, Shanghai, China. E-mail: {lguo2014@sjtu.edu.cn, zhaiguangtao@sjtu.edu.cn}.

Manuscript received April 19, 2005; revised August 26, 2015.

able results on a wide range of video analysis tasks.

As for the specific instantiation, we first build a simple Semantic-Mining-then-Compensation (SMC) model, which compensates and amends the semantic loss problem of current lossy video codecs. Specifically, the semantic features of the original video and the lossy video are extracted on the encoder side, and only the residual semantics is compressed by a convolutional neural network. During decoding, the residual-compensated semantic feature is synthesized as the videos, deployed for various AI tasks.

Furthermore, we extend the SMC model to a more advanced SMC++ model from the following aspects:

First, we augment the masked learning task by additionally predicting motion. Motion is another critical cue in videos, which benefits a series of video tasks. For example, motion information is necessary for discriminating the visually-ambiguous actions [34]. Therefore, we introduce another decoder to the MVM task header, for predicting the motion targets of the masked regions, expecting to enhance the temporal semantic modeling capability of our framework.

Second, we improve the coding efficacy by introducing a Blueprint-guided compression Transformer (Blue-Tr). The basic SMC model adopts simple convolution operations for compression, which can not adequately model complex semantic redundancies. The self-attention [35] operation is more powerful, but still faces challenges in capturing redundancies among heterogeneous features, which are distributed in various coding stages of the compression system. To address this issue, we propose a multi-step “Blueprint mining-feature aligning-redundancy modeling” approach. First, we mine the most critical semantic part of the current frame, which we call blueprint semantics. Subsequently, we employ the blueprint to align diverse heterogeneous features that are distributed in different timestamps and coding layers. Finally, given the aligned features, a decomposed Transformer model is adopted to capture the semantic redundancies. Our contributions are:

- We propose the first masked learning framework for the unsupervised video semantic compression problem, aiming to better support various semantic analysis tasks under low-bitrate conditions. This framework is instantiated as a simple SMC model.
- We devise the Non-Semantics Suppressed (NSS) learning strategy to better adapt the general masked learning scheme to the compression problem, aiming to suppress the encoding of non-semantic information.
- We further extend SMC as SMC++ by introducing 1) a masked motion modeling objective and 2) a new Blueprint-guided compression Transformer (Blue-Tr), for 1) learning better temporal semantics and 2) compressing semantics more effectively. The newly proposed Blue-Tr introduces a blueprint semantics concept, and uses it to align diverse features. The aligned features are easier to compress, fully unleashing the power of the Transformer-based compression module.
- The proposed models SMC and SMC++ demonstrate notable superiority over previous traditional, learnable, and perceptual codecs, on three video analysis tasks and seven datasets. Moreover, we append SMC++ with a small detail rendering network. The resulting

SMC++* model achieves superior visual detail coding performance, on four video compression datasets.

This work extends our preliminary conference version [36] with the following substantial improvements. 1) We provide more analysis and visualization results of the masked learning procedure and the proposed NSS strategy, aiming to help readers more intuitively understand their effectiveness in the context of video semantic compression. 2) We introduce an additional masked motion prediction term to the original appearance-only MVM task loss. We compare and analyze the impact of different motion target choices. 3) We propose a Blueprint-guided compression Transformer (Blue-Tr) for more effective semantic compression. We perform ablation studies and detailed analysis for our proposed Blue-Tr. 4) The above two improvements lead to the advanced SMC++ model, which remarkably outperforms the most recent semantic coding approach VCS [37] and neural video codec DCVC-FM [38]. We also compare recent approaches under a more advanced compression setting, *i.e.*, group-of-picture(GOP) size of 32. 5) We append the SMC++ model with a lightweight decoder, obtaining a PSNR-oriented model SMC++*. SMC++* surpasses the advanced VTM20.0 software [39] by a notable margin, in both low-delay P (LDP) and random access (RA) test conditions.

The rest of the paper is organized as follows. In Section 2, we give a brief review of the related works. In Section 3, we outline our masked learning-based video semantic coding framework, then instantiate it as two specific models. Finally, we report the experimental results and conclude the paper in Section 4 and Section 5, respectively.

2 RELATED WORKS

Video Compression. Previous video codecs, including traditional ones [40] [1] [2] [41], learnable ones [42] [3] [4] [43] [44] [45] [46] [42] [47] [48] [38] and mixed ones [49] [50] [51], are designed to achieve better pixel-wise signal quality metrics, *e.g.*, PSNR and MS-SSIM [52], which mainly serve the human visual experience. Recently, there are also some generative video coding methods [53] [54] that mainly consider visual comfort and perceptual quality. Despite recent methods achieving significant strides in low-level visual metrics like PSNR and SSIM, their effectiveness on semantic AI tasks is still undesirable [6]. This prompts the research on the video semantic compression problem.

Video Coding for Machine (VCM). Early standards such as CDVA [12] and CDVS [11] [10] propose to pre-extract and transport the image keypoints, supporting image indexing or retrieval tasks. Some works [7] [8] [9] [16] [17] [18] [19] [20] compress the intermediate feature maps instead of images. Besides, some works [13] [14] [15] [55] [56] [57] [58] improve traditional codecs by introducing downstream task-guided rate-distortion optimization strategy or another task-specific feature encoding stream [59] [8]. Also, some methods [60] [61] [62] [63] [26] optimize the learnable codecs by directly incorporating the downstream task loss. Recently, some methods exploit hand-crafted structure maps [64] [65] for semantic coding. To summarize, most above methods rely on task-specific labels or hand-crafted priors, which may not be generalizable enough.

Recently, some works have leveraged self-supervised representation learning methods for learning a compact semantic representation. As a pioneering work, Dubois *et al.* [66] theoretically revealed that the distortion term of the lossy rate-distortion trade-off for image classification can be approximated by a contrastive learning objective [67]. However, the compressed semantics are empirically effective to a group of tasks that share a similar prior (*i.e.*, labels are invariant to data augmentations), but may severely discard the semantics useful to other tasks such as detection and segmentation. Feng *et al.* [20] proposed to learn a unified feature representation for AI tasks from unlabeled data in a similar manner. In these methods, the downstream models are required to be fine-tuned to adapt to the features.

Our previous work [37] presented a one-bit semantic map that efficiently compresses video semantics into a compact space, advancing semantic compression. Nonetheless, it faces certain restrictions. Firstly, the one-bit semantic map was heuristically hand-designed, based on the assumption that image edges retain most semantics, such as object structures. This work eliminates such human-derived priors. Secondly, the previous approach relies on contrastive learning, which is inferior to the masked learning technique adopted in this work, as evidenced in numerous papers.

Scalable Coding and Visual-Semantic Fusion Coding. Scalable coding methods [64] [23] [22] [24] [25] [56] can achieve excellent compression efficiency when measured with the trained tasks, but usually show undesirable results on the tasks/data out of the training scope, due to the supervised learning paradigm. Visual-semantic fusion coding methods [65] [68] [69] [64] [70], *a.k.a.*, conceptual coding [71] [72] [73] [74], first extract the structure information and the texture information on the encoding side, and then fuse the two parts into an image on the decoding side. The fused images are readily fed into various tasks and achieve superior performance even at low bitrate levels. However, almost all these methods employ semantic segmentation map [65] or edge map [64] as the semantic stream, not fully discarding the task-specific priors.

Compressed Video Analysis. There are also amounts of works such as [75] [76] [77] [78] [79] [80] perform video analysis tasks, such as action recognition [81] [82] [83] [84] [85] [86] and multiple object tracking (MOT) [87] [88], in the compressed video domain. However, these methods focus on developing video analysis models that better leverage the partially decoded video stream, such as the motion vector. In contrast, our work focuses on the coding procedure.

Self-Supervised Semantic Learning. Recent methods can be mainly divided into two categories, *i.e.*, Contrastive Learning (CL) ones [67] [89] [90] [91] and Masked Image Modeling (MIM) ones [92] [31] [32] [33]. CL methods use two augmented views of the same image as the positive pair, and other images as negative samples. The learned semantics relies on the employed augmentation strategy [93], and is usually biased to global semantics. Recently, MIM methods have gained increasing attention. MIM simply predicts masked patches from unmasked ones, while showing remarkably strong performance in downstream tasks. After the pioneering works, *e.g.*, MAE [31] and Beit [94], amounts of works are proposed to improve the MIM framework [95] [96] [33] or the prediction target [97] [92] [98].

Although MIM methods are superior to CL ones in many aspects, when the masked region reconstruction loss serves as the semantic learning objective of a compression system, it also facilitates the system encoding some non-semantic information, and wasting extra bitcosts. Our work solves this problem by explicitly suppressing the non-semantics information within the MAE feature space. Very recently, there are some works [99] [100] extending VideoMAE [32] with motion prediction targets, achieving superior results on video action recognition task. In this work, we also incorporate this motion-based target into our system, verifying its effectiveness on the video semantic compression problem.

3 APPROACH

3.1 Framework Overview

The proposed masked learning-powered video semantic coding framework is shown in Figure 1. Let the original video X and its lossy version \tilde{X} , which is compressed by a lossy video codec such as VVC. On the encoder side, we extract the semantic information from the original video and the lossy video, respectively. Then, the original video semantics is compressed with the aid of the lossy semantics. On the decoder side, we fuse the reconstructed semantic feature \hat{S} and the lossy video \tilde{X} as the video \hat{X} , which is deployed to support various machine analysis tasks.

The framework is optimized via a non-semantics suppressed Masked Video Modeling (MVM) objective. The framework sub-components are detailed as follows.

Semantic Extraction Network (Sem-Net). To transform the videos from RGB space to semantic space, the original video X and the lossy video \tilde{X} are encoded as the semantic features S and \tilde{S} , respectively. The tensor shape of S and \tilde{S} are both $\mathbb{R}^{T \times 512 \times \frac{H}{32} \times \frac{W}{32}}$, where T and $H \times W$ represent the temporal length and spatial dimensions of the input video. For producing S , we adopt the ResNet18 [101] network as the Sem-Net, but replace its first Max-pooling layer with a stride two convolution layer for retaining more information. For producing \tilde{S} , we adopt a more lightweight network denoted Sem-Net_s, since it has to be performed twice on both the encoder and decoder sides. Sem-Net_s mainly consists of five convolution layers of stride size two and kernel size three. We also insert depth-wise convolutions of large kernel size 7×7 to effectively enlarge the receptive field size, without substantially increasing the computational cost. The weights of the above two networks are randomly initialized.

Semantic Coding. In the basic model SMC, the residual semantic feature Res between the original video feature S^t and lossy one \tilde{S}^t will be computed by a simple subtraction operation, and then compressed with an auto encoder-decoder CNN network, as shown in Figure 1 (c). Adding back the reconstructed residual semantic feature to \tilde{S}^t , we produce the compensated semantic feature \hat{S}^t . Both the encoder and the decoder networks, *i.e.*, Sem-Enc and Sem-Dec, are composed of three residual blocks [101].

The above residue-based compression strategy only exploits the simple local redundancies, neglecting both long-range spatial redundancy and temporal redundancy. In the improved SMC++ model, we employ the self-attention mechanism to model the spatial-temporal redundancy among current semantics S^t , previous semantics

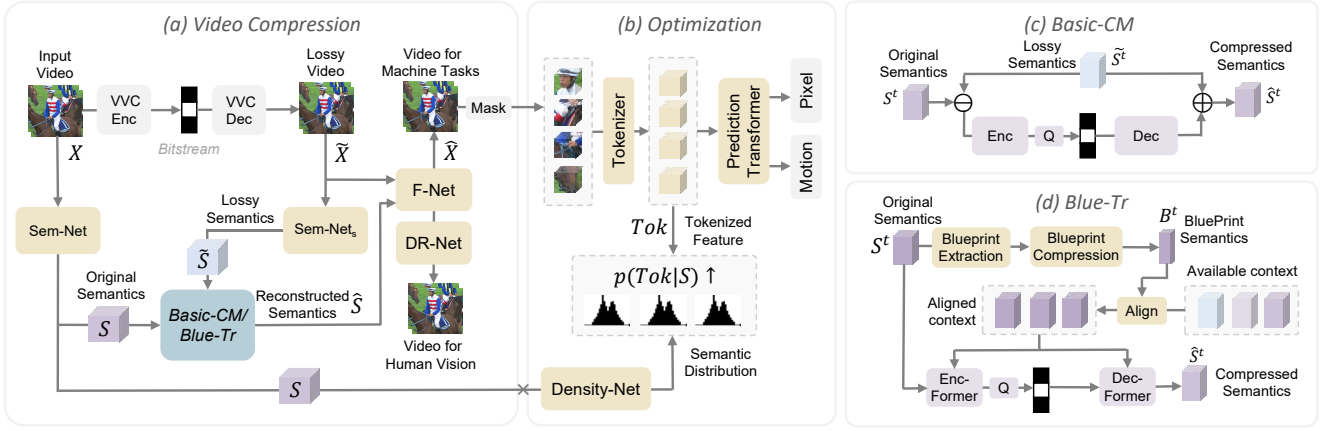


Fig. 1: Framework overview. First, the semantic features of the original and the lossy videos are separately extracted by Sem-Net. Then, the original semantic feature is compressed with the aid of the lossy semantic by Basic-CM/Blue-Tr. Finally, the reconstructed semantic feature and the lossy video are fused by F-Net, generating the semantically-sound video that supports various analysis tasks. The framework is optimized via a non-semantics suppressed Masked Video Modeling (MVM) objective. In the basic model SMC, the MVM task only predicts the pixels, meanwhile the semantics is compressed by a simple residue-based compression module (Basic-CM). In the improved model SMC++, a motion-prediction MVM objective is further incorporated for better temporal semantic modeling, and a powerful Blueprint-guided compression Transformer (Blue-Tr) is introduced. \times denotes the gradient-stopping operation. Q denotes the quantization operation. Our framework can further support high-fidelity video decoding, by appending a detail rendering network (DR-Net).

S^{t-1} , current lossy semantics \tilde{S}^t and previous lossy semantics \tilde{S}^{t-1} , where lossy semantics is extracted from the lossy video compressed by the base VVC layer. However, it is not trivial to directly model the redundancy among these highly heterogeneous features. For example, the features S^t and \tilde{S}^{t-1} of different timestamps are not spatially aligned. The features S^t and \tilde{S}^t extracted from original and lossy videos exhibit domain gap. To address this issue, we introduce the blueprint semantic feature to align the above features in terms of both spatial arrangement and domain. The aligned features are then compressed by a pair of encoding and decoding Transformers, as shown in Figure 1 (d).

Semantic-Visual Information Fusion. After obtaining the reconstructed semantic feature \hat{S} and the lossy video \hat{X} on the decoder side, we use a UNet-style [102] generator network termed F-Net to synthesize the final video \hat{X} , which will be consumed by downstream AI task models. Considering that global structures instead of local details are more critical to video semantics, the above feature fusion procedures within the UNet are conducted in four-, eight-, and sixteen-times downsampled feature spaces.

High-Fidelity Decoding Support. In practical applications, videos serve a dual purpose: machine task support and human viewing. To ensure our framework can decode high-fidelity details suitable for human inspection, we further append it with a lightweight Detail Rendering Network (DR-Net). The decoded high-fidelity videos also allow for the manual review of AI analysis results.

3.2 Semantic Learning Objective

In this section, we describe how to learn compressible semantic representation from unlabeled videos, which is one of the core challenges for the unsupervised semantic coding problem. The learning objective is based on the MAE framework [31], inspired by the fact that MAE learns strong and generalizable semantic representation from unlabeled

image/video data. Furthermore, to improve the semantic coding efficiency, *i.e.*, excluding semantic-less information for saving bitcost, we introduce a Non-Semantics Suppressed (NSS) learning strategy to better adapt the vanilla MAE objective to the coding problem.

MAE Learning. Given the decoded video \hat{X} , we first divide it into regular non-overlapping patches of size 16×16 , and each patch is transformed to tokens by linear embedding. Then, a proportion of tokens are randomly masked, and the remaining unmasked token set Tok is fed into the prediction network ϕ , which includes an encoder and a decoder, for reconstructing the video. The pixel-wise reconstruction loss of the MAE task is given by,

$$\mathcal{L}_{MAE-pixel} = \frac{1}{\mathcal{M}} \sum_{i \in \mathcal{M}} |\phi(Tok)[i] - X[i]|, \quad (1)$$

where i is the masked token index, \mathcal{M} is the index set of masked tokens, and X is the ground-truth video, $|\cdot|$ denotes the ℓ_1 distance function. We adopt the ℓ_1 instead of the patch-normalized ℓ_2 [31] [32], as we prefer the stable gradient values 1 of ℓ_1 . This stabilizes the joint training with other loss functions in our system, such as GAN loss.

Furthermore, considering that temporal dynamics, *e.g.*, motion information, is another crucial component of videos, we also extend the MAE learning objective from the above pixel-only one to a motion-enhanced one,

$$\mathcal{L}_{MAE-motion} = \frac{1}{\mathcal{M}} \sum_{i \in \mathcal{M}} |\mathcal{T} \cdot \phi_m(Tok)[i] - \mathcal{T} \cdot X[i]|, \quad (2)$$

where ϕ_m shares the parameters of the encoder with ϕ but includes a motion decoder that is not shared. \mathcal{T} denotes the motion calculation function, such as the pixel-wise difference map, the optical flow map, and the feature-wise correlation map. In the experimental section, we extensively compare these design choices.

Guided by the above objectives, the shared encoder implicitly clusters the video patches into some semantic centers, and the decoder builds a spatial-temporal reason graph among these semantic primitives to predict the pixels or motions of the masked region. This facilitates preserving semantics-relevant information within each patch of the compressed video, as well as interactions among different patches. However, these detail-reconstruction objectives also encourage \hat{X} over-memorizing some non-semantic information, such as the object texture details, which degrades the quality of the learned semantic representation, as well as decreases the compression efficiency.

Non-Semantics Suppressed (NSS) Learning. To suppress the non-semantic information leaked from X to the compressed video \hat{X} , we explicitly regularize the information entropy of the tokens Tok in MAE feature space, conditioned on the mined semantic feature S . However, due to the difficulty of estimating the entropy of a continuous variable, we insert a quantization operation in the tail of the tokenization procedure, so that Tok is a discrete variable. Then, we use a Gaussian Mixture Model (GMM) [103] with component number K to approximate its distribution. The distribution of each token $Tok(i)$ is defined by the dynamic mixture weights w_i , means μ_i and log variances σ_i , which are produced by a density parameter estimation network (Density-Net). With these parameters, the distributions can be determined as,

$$p(Tok[i]|S) \sim \sum_{k=1}^K w_i^k \cdot \mathcal{N}(\mu_i^k, e^{\sigma_i^k}). \quad (3)$$

Then, the discretized likelihoods of each video patch token can be given by,

$$p(Tok[i]|S) = c(Tok[i] + 0.5) - c(Tok[i] - 0.5), \quad (4)$$

where $c(\cdot)$ is the cumulative function [104] of the GMM in Equation 3. Finally, the non-semantics suppressed mask learning objective can be given by,

$$\mathcal{L}_{Sem} = -\beta \log(p(Tok|S)) + \mathcal{L}_{MAE}, \quad (5)$$

where β is the balancing weight.

In our basic SMC model, \mathcal{L}_{MAE} is pixel-based reconstruction loss $\mathcal{L}_{MAE-pixel}$ for simplicity. In our improved SMC++ model, \mathcal{L}_{MAE} incorporates both the pixel- and the motion-based reconstruction objectives, *i.e.*, $\mathcal{L}_{MAE} = \frac{1}{2}\mathcal{L}_{MAE-pixel} + \frac{1}{2}\mathcal{L}_{MAE-motion}$, aiming to learn enhanced spatial-temporal representation capability.

Discussion. Although Equation 4 shares a similar format with the bit estimation procedure of the hyper-prior-based image compression methods [105] [106], our goal is fundamentally different from theirs. Our approach aims to suppress the extra non-semantic information that is introduced by the MAE task, transporting zero bits, while the method [105] explores the hierarchical redundancies within images, and the estimated bits are additionally transported.

We further visualize the patch features, aiming to intuitively illustrate how the entropy regularization item of NSS improves the effectiveness of the semantics learned by MAE. First, we randomly select one hundred videos from the UCF101 dataset. Then, we cluster the patch features of these videos into individual groups using the

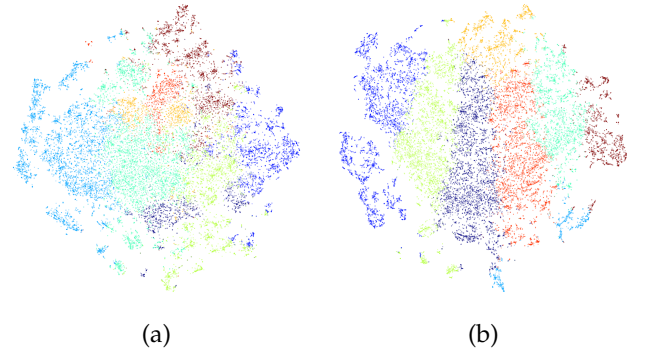


Fig. 2: Visualization of the patch features learned by different semantic objectives, *i.e.*, (a) vanilla MAE loss \mathcal{L}_{MAE} and (b) our non-semantics suppressed MAE loss \mathcal{L}_{Sem} .

K-Means algorithm [107]. The cluster ID is then utilized as the pseudo-category for each patch. Subsequently, the features are visualized using the t-SNE technique [108]. As compared in Figure 2, although the vanilla MAE loss can learn roughly separable semantic representation, our non-semantics suppressed loss \mathcal{L}_{Sem} learns much clearer semantic boundaries, indicating less semantic noises. This also saves the semantic bitcost (0.0074bpp *v.s.* 0.0028bpp for \mathcal{L}_{MAE} and \mathcal{L}_{Sem} , respectively).

Density-Net. It consists of two stacked convolutions of kernel size three, aligning the semantic feature S to the MAE feature space. Then, we append a multiple layer perceptron (MLP) to predict w , μ , and σ within Equation 3. The gradient of S is detached during the back-propagation procedure, forming a self-bootstrapping paradigm and avoiding the collapsing solution [109]. NSS scheme enforces the masked learning procedure to focus on mining semantic information, while the optimized semantic-rich S leads to a more principled NSS objective.

3.3 Overall Optimization Target

The overall optimization target is to enforce the decoded video \hat{X} of rich semantics and good visual quality, while minimizing the bitrate of the transported semantic feature. The whole loss function can be given by,

$$\mathcal{L} = \alpha \mathcal{L}_{Sem} + \mathcal{L}_{lpips} + \mathcal{L}_{GAN} + H, \quad (6)$$

where α is the balancing weight. Following [110], we introduce the combined $\mathcal{L}_{lpips} + \mathcal{L}_{GAN}$ item to regularize the visual quality of the compressed video, where \mathcal{L}_{lpips} denotes the perceptual loss [111], and \mathcal{L}_{GAN} denotes the GAN loss. H represents the semantic feature bitrate, which is estimated with the factorized bitrate estimation model [112].

3.4 Blueprint-Guided Compression Transformer

In this section, we introduce another new component of the SMC++ model, *i.e.*, Blueprint-guided compression Transformer (Blue-Tr), which effectively captures redundancy among heterogeneous features across different frames and coding layers. As illustrated in Figure 3, Blue-Tr operates under an “align-then-compress” paradigm, guided by a novel blueprint semantic representation. The compression procedure consists of the following three steps:

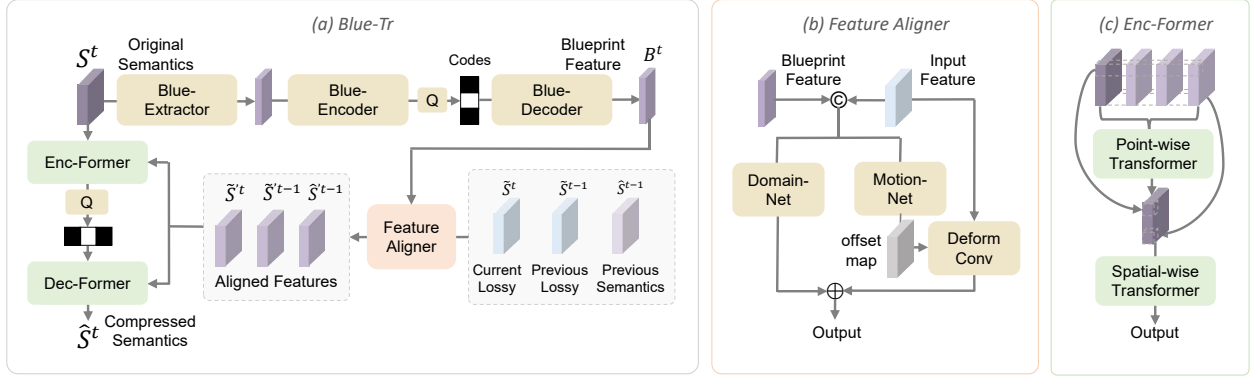


Fig. 3: Blueprint-guided compression Transformer (Blue-Tr) first extracts a blueprint semantic feature, which is then employed to align diverse available features. Finally, a decomposed Transformer compresses redundancies among the current frame’s semantic feature and the aligned features. The feature aligner module (b) align different features by using the blueprint feature as the guidance. Q denotes the quantization operation. The current lossy semantics \tilde{S}^t is also fed into the Blue-Encoder/Decoder for aiding the compression of the blueprint feature. We omit this in the figure for simplicity.

Blueprint Semantic Extraction and Compression. Drawing inspiration from coarse-to-fine compression approaches [113] [114], we extract the most salient video feature component, termed the blueprint semantic feature, as the coding guidance. Instead of downsampling the spatial dimension as in previous works, we condense the channel dimension for extracting the salient semantics, since semantic information is mostly encoded in the channels [115]. Specifically, given the current frame’s semantic feature S^t , we employ a Blue-extractor network to produce the blueprint feature with a channel dimension one-fourth that of S^t . This blueprint feature is then compressed using a pair of lightweight CNN-based compression networks, resulting in the compressed blueprint feature B^t , which is available at both the encoder and decoder to aid in compressing S^t .

The Blue-extractor network consists of three convolution layers with gradually decreasing channel number. Its first two convolutions are followed by a residual block to enhance the non-linear transformation capability. The encoder of the compression network is the same as the Blue-extractor network, while the decoder part is symmetric to the encoder. Besides, \tilde{S}^t is together fed into the encoder and decoder network to reduce the blueprint feature bitcost.

Feature Alignment. Existing learnable video compression networks typically leverage motion information to compensate for the previous frame. The produced frame is mostly aligned with the current frame, serving as an effective coding reference. However, our framework goes beyond just the previous frame, additionally involving the (current and previous) lossy frames from the base VVC coding layer. Therefore, we use the blueprint feature B^t to align all these features simultaneously in a unified manner.

As shown in Figure 3 (b), the alignment operation includes two branches: one for motion compensation and another for domain correction. The motion branch estimates the motion between the input feature and B^t using a Motion-Net and aligns their spatial arrangements via deformable convolution [116]. The domain branch uses a Domain-Net to correct the input feature domain. The features from both branches are subsequently fused. Both Motion-Net and Domain-Net comprise three convolution layers equipped with the LeakyReLU [117] activation.

Contextual Compression. Leveraging the aligned current lossy feature, aligned previous lossy feature, and aligned previous semantic feature as coding context, we compress the current semantic feature S^t in an contextual coding manner [4]. During encoding, we feed these context features and S^t together into an Enc-Former, generating a compressed feature. This feature is then quantized and encoded into bitcodes. On the decoder side, the compressed feature is fed into a Dec-Former together with context features, to reconstruct the semantic feature \hat{S}^t .

Due to the previous alignment step, features at corresponding spatial locations exhibit high correlation. Consequently, the Enc-Former adopts a decomposed architecture: a point-wise Transformer eliminates redundancy across different features, followed by a spatial-wise Transformer to reduce spatial redundancy. This strategy significantly reduces the computational cost of the self-attention operation, approximately $\frac{1}{N^2}$ compared to the vanilla one, where $N = 4$ is the type number of features fed into the Transformer. As the feature types expand, for example, by increasing the previous frame number, the cost reduction can be further improved. Dec-Former mirrors the Enc-Former’s architecture. Each Transformer includes three self-attention blocks [35].

Discussion. Our approach inherits the strengths of two popular neural coding paradigms: motion-based explicit modeling approaches such as FVC [3], and Transformer-based implicit modeling approaches like VCT [118]. Similar to FVC, we warp feature maps and align features across timestamps. However, our Transformer-based approach excavates more intricate redundancies between features at different timestamps, positions, and coding layers. Compared to VCT, we incorporate motion modeling to guide the Transformer, simplifying optimization and enhancing the model’s robustness against large motion.

3.5 High-Fidelity Decoding Support

To serve human viewing, we introduce the Detail Rendering Network (DR-Net) to fuse the videos from our framework and the base VVC layer, yielding high-fidelity video output. Note that this procedure does not involve transporting any new information, since our framework is built upon the

VVC codec, and decoding the VVC-compressed video is an intermediate step of our approach.

The fusion procedure comprises three sub-steps: 1) *Intra-semantic fusion*: Given the semantic-rich video from SMC++, an encoder network extracts features from each frame. The previous frame features are aligned to the current one with the Feature Aligner in Figure 3 (b), producing the fused semantic feature. 2) *Intra-lossy fusion*: This step is similar to the above procedure, except the input frames are from the VVC layer, producing the fused lossy feature. 3) *Pixel decoding*: The above fused features are concatenated, and then fed into a decoder network to generate the final frames.

The encoder network comprises two stride-two convolution layers, succeeded by three residual blocks. The decoder network is symmetric with the encoder network. All convolution layers have 64 channels. We optimize DR-Net using the ℓ_1 loss between the generated and original frames. The parameters within SMC++ are frozen during the optimization, so that most inference costs can be shared for decoding semantic-rich videos and detail-rich videos.

4 EXPERIMENTS

4.1 Evaluation Datasets

For action recognition task, we evaluate on four large-scale video datasets, UCF101 [119], HMDB51 [120], Kinetics [83], and Diving48 [121]. For multiple object tracking (MOT) task, we evaluate on MOT17 [122]. For video object segmentation (VOS) task, we evaluate on DAVIS2017 [123]. We also compare the compression performance on Standard HEVC Test Sequences [1], including HEVC Class B/C/D/E datasets.

Dataset Processing. During the training procedure, we randomly select 60K videos of resolution larger than 1280×720 from the training set of Kinetics400, following the previous approach [37]. The quantization parameter (QP) value of VVC is randomly sampled, so that the framework is learned to adapt to various QPs with a single model. To reduce the training time cost, we pre-compress the training videos with various QP and buffer these compressed videos in an offline manner, so that the time-consuming video compression procedure can be eliminated.

For the evaluation of *action recognition* datasets, we first downsample the shortest side of the video to 256 pixels and then crop it to the size 224×224 before the coding procedure. For the evaluation of *MOT*, we adopt the original MOT17 dataset without downsampling, since many tracking methods require high-resolution inputs. For the evaluation of *VOS*, we download the high-resolution version of DAVIS2017, which contains videos from 720p to 1080p, and then downsample them to 480p (854×480), which is the input resolution of most VOS methods.

4.2 Experimental Setting

Downstream Task Models. For the *action recognition* task, we adopt the following popular models, i.e., TSM [124], SlowFast [125], and TimeSformer [126], including 2D CNN, 3D CNN and the recent Transformer architectures. The model weights are provided by the MMAction2 framework [127]. For the *MOT* task, we adopt ByteTrack [128], of which the model weights are provided by MTrack-ing [129]. For the *VOS* task, we adopt XMem [130], of which

the model weights are officially released by the authors. We emphasize that we directly feed the decoded videos by our framework into these official models, without fine-tuning them, since fine-tuning the numerous downstream video models for the codec is not practical in real-world applications. The adopted models are right the same as VCS [37], as we prefer a completely fair comparison.

Baseline Codecs. HEVC is evaluated with FFmpeg software [131] and x265 codec. VVC is evaluated with VVenC1.5.0 software [132], which consumes much less encoding time than the VVC reference software VTM, so that supporting the evaluation of large-scale video datasets containing thousands of videos. FVC [3] is a representative work on learnable codec. PLVC [53] is a recent perceptual quality-oriented codec. DCVC-FM [38] is the state-of-the-art neural video codec. VCS [37] is the state-of-the-art semantic video compression method. For traditional codecs, the QP value is selected from $\{51, 47, 43, 39, 35\}$, as setting QP to larger values does not degrade the downstream task obviously. All codecs and our framework are evaluated on Low-Delay with P frame (LDP) coding mode. Both VCS and our models SMC and SMC++ are built upon the VVenC1.5.0 software, for a fair comparison.

Evaluation Metrics. We use bpp (bit per pixel) to measure the average number of bits used for one pixel in each frame. For the *action recognition* task, we adopt the Top1 accuracy as the performance indicator. For the *MOT* task, we adopt MOTA (multiple object tracking accuracy) [133], MOTP (multiple object tracking precision), FN (false negative detection number), and IDF1, which is the ratio of correctly identified detections over the average number of ground truth and computed detections. For the *VOS* task, the standard metrics Jaccard index \mathcal{J} , contour accuracy \mathcal{F} and the average of \mathcal{J} and \mathcal{F} ($\mathcal{J} \& \mathcal{F}$) are adopted. We also report the contour recall \mathcal{F} -Recall.

Implementation Details. Following VideoMAE [32], the masking ratio for the MAE task is set to 90%, where the encoder and decoder networks consist of six and two ViT blocks [134] with divided space-Time attention [126], respectively. Following previous works [135] [84] on video temporal modeling, we also insert temporal convolutions with kernel size 3 before each 3×3 convolutions of bottleneck layers of the original ResNet18 encoder network, aiming to enhance its basic temporal modeling ability. The temporal convolutions are implemented using causal convolutions [136]. In this design, only the historical information is accessible, with the intention of preserving the P-frame coding mode setting. The weights of all networks within our framework are randomly initialized.

K in Equation 3 is empirically set as 5. α and β are set to 1 and 0.1, respectively. The resolution of training videos is 256×256 and the clip length is 8. We use the Adam optimizer [137] by setting the learning rate as 1×10^{-4} , β_1 as 0.9 and β_2 as 0.999, respectively. The learning rate is decayed to 1×10^{-5} in the last 100k iterations. The training iteration number of SMC is 1000k. The mini-batch size is 24. To ensure that the encoder begins with a well-initialized state, we omit the quantization step for the initial 100k iterations. This allows precise gradient values to be propagated back to the encoder side. The system is implemented with Pytorch [138] and it takes about six days to train the SMC

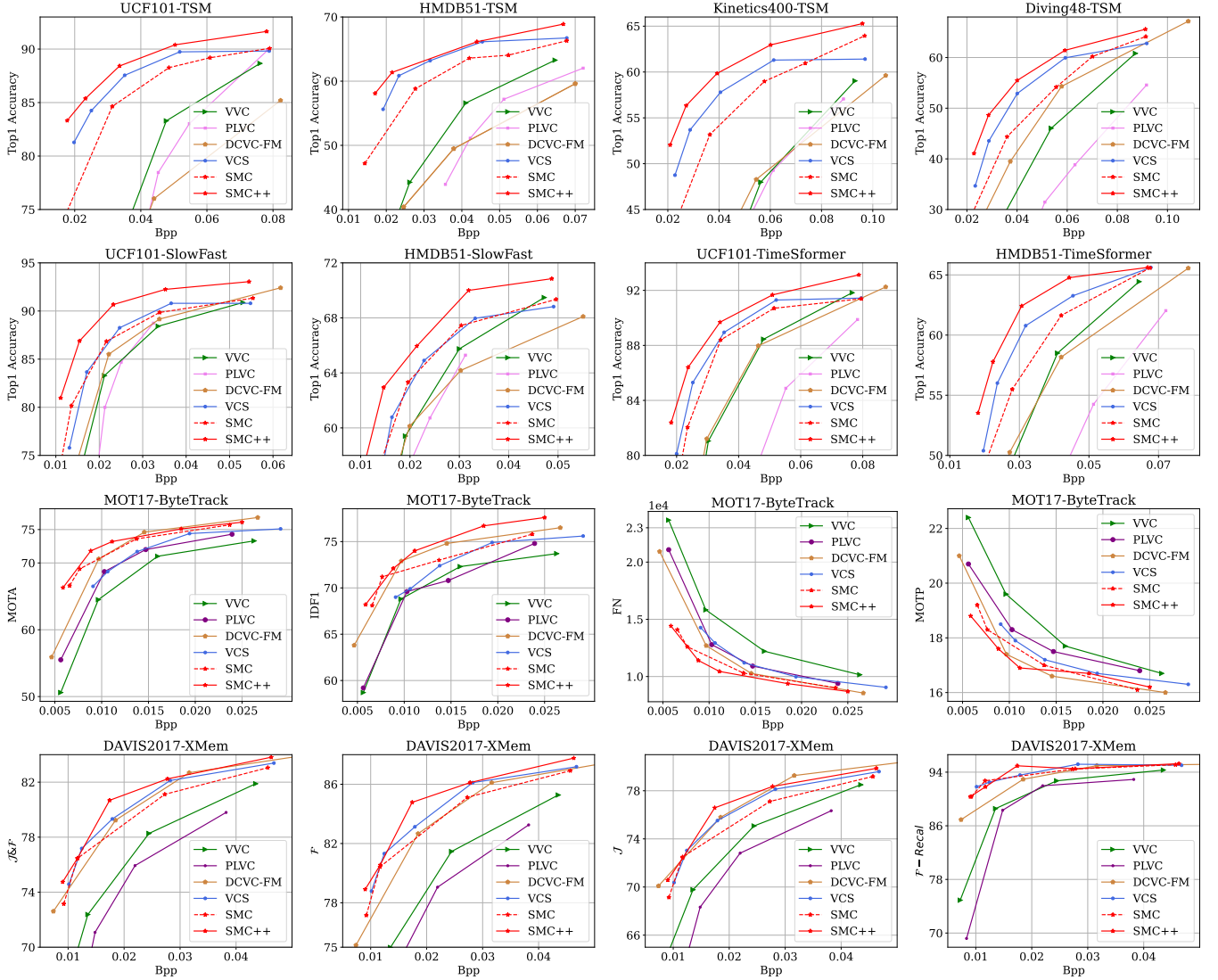


Fig. 4: Semantic coding performance on Action Recognition (1st and 2nd rows), VOS (3rd row), and MOT (4th row) tasks. The plot titles are in {Dataset}-{Task Model} format. The codec setting is LDP mode with GOP size 10.

model using eight Nvidia 3090Ti GPUs. The SMC++ model is initialized from the SMC model and trained by another 500,000 iterations. The learning rate is set to 1×10^{-4} in the first 400,000 iterations and decayed to 1×10^{-5} in the last 100,000 iterations. The additional training procedure of SMC++ takes about six days with eight Nvidia 3090Ti GPUs.

4.3 Experimental Results

Action Recognition. In Table 1, we evaluate various video compression methods on the action recognition task. Our basic SMC model remarkably outperforms traditional codecs HEVC and VVC, the learnable codecs FVC and DCVC-FM, and the perceptual codec PLVC. For example, on the UCF101-TSM setting, our SMC model shows 22% and 10% Top1 accuracy improvement over FVC and VVC, respectively, at 0.04bpp. On the HMDB51-TSM setting, SMC outperforms the DCVC-FM by 18% at 0.03bpp. Although the most recent semantic coding approach VCS surpasses our basic SMC model, our enhanced SMC++ model outperforms it again, notably with over 5% Top1 accuracy gain on the Diving48-TSM setting at 0.03bpp. Moreover, on the

large-scale Kinetics400 dataset, our SMC++ model surpasses VCS and DCVC-FM by 1.86% and 13.42% Top1 accuracy, respectively, at 0.06bpp. When being evaluated with the Slowfast and TimeSformer action recognition networks, our SMC++ model still outperforms all other approaches by a large margin, *i.e.*, about 4% Top1 gain over VCS at 0.02bpp.

We present the rate-performance (RP) curves of recent coding methods in the 1st and 2nd rows of Figure 4. Our SMC++ model leads all other methods across all datasets and bitrate levels. Our basic SMC model also excels, outperforming all except VCS. Interestingly, we observe that the state-of-the-art neural codec DCVC-FM shows unsatisfactory performances, *e.g.*, it even underperforms VVC on the HMDB51-TSM and Kinetics400-TSM settings, despite having superior PSNR performance [38] compared to the successor of VVC, *i.e.*, the ECM software [139]. This suggests that the recent neural codecs may be overfitting to the standard HEVC test sequences, as its hyperparameters are manually tuned for these sequences.

Multiple Object Tracking (MOT). Beyond action recognition, we evaluated our coding approach on the more challenging Multiple Object Tracking (MOT) task, demand-

TABLE 1: Results on action recognition. “Original” denotes the performance upper-bound, which is evaluated on the original dataset. The codec setting is LDP mode with GOP size 10.

	TSM Top1 (%)					Slowfast Top1 (%)			TimeSformer Top1 (%)		
	UCF101	HMDB51	Kinetics400	Diving48	Diving48	UCF101	HMDB51	HMDB51	UCF101	UCF101	HMDB51
Bpp	@0.04	@0.04	@0.06	@ 0.03	@ 0.05	@0.03	@0.02	@0.03	@0.02	@0.04	@0.04
HEVC	52.70	36.64	35.28	-	22.48	85.13	47.78	62.68	47.16	69.92	37.45
FVC	64.61	47.54	37.23	-	22.94	79.43	52.15	59.81	58.90	72.47	45.11
PLVC	71.40	48.67	48.65	-	30.13	87.38	56.33	64.50	38.92	70.06	44.59
VVC	76.97	55.72	49.11	24.38	42.75	86.93	59.95	65.74	66.98	85.10	57.83
DCVC-FM	72.71	50.15	49.51	32.16	48.67	87.95	60.15	64.06	69.50	85.39	57.08
VCS	88.19	64.98	61.07	44.57	56.54	89.39	63.09	67.01	80.11	89.60	62.27
SMC	86.46	62.92	59.26	37.79	51.36	88.89	63.48	67.30	77.61	89.17	60.74
SMC++	89.17	65.29	62.93	49.45	58.58	91.56	65.33	69.27	83.66	90.39	64.02
Original	93.97	72.81	70.73	75.99	75.99	94.92	72.03	72.03	95.43	95.43	71.44

TABLE 2: MOT performance comparison of different coding methods on MOT17. The codec setting is LDP mode with GOP size 10. “Original” denotes the results with original videos, *i.e.*, the performance upper bound.

Bpp	@0.01bpp		@0.015bpp		@0.02bpp	
	MOTA(%)	IDF1(%)	MOTA(%)	IDF1(%)	MOTA(%)	IDF1(%)
HEVC	61.30	64.32	68.61	69.62	71.90	72.18
FVC	44.24	52.53	51.84	58.61	59.43	64.68
PLVC	67.87	68.95	72.07	70.92	73.31	73.09
VVC	64.86	68.99	69.99	71.75	71.89	72.84
DCVC-FM	70.85	73.02	74.68	74.86	75.58	75.56
VCS	67.79	69.53	72.28	72.93	74.44	74.94
SMC	70.84	71.89	73.86	73.35	74.92	74.76
SMC++	72.51	73.07	74.19	75.41	75.33	76.90
Original	78.60	79.00	78.60	79.00	78.60	79.00

TABLE 3: VOS performance comparison of different coding methods on DAVIS2017. The codec setting is LDP mode with GOP size 10. “Original” denotes the results with original videos, which is the performance upper bound.

Bpp	@0.01bpp		@0.02bpp		@0.03bpp	
	$\mathcal{J}\&\mathcal{F}$ (%)	\mathcal{F} (%)	$\mathcal{J}\&\mathcal{F}$ (%)	\mathcal{F} (%)	$\mathcal{J}\&\mathcal{F}$ (%)	\mathcal{F} (%)
HEVC	57.68	58.51	73.28	75.96	77.45	80.56
FVC	62.39	63.55	75.87	68.85	71.68	74.15
PLVC	61.45	62.87	74.60	77.62	77.84	81.13
VVC	67.47	69.36	75.87	78.82	79.32	82.57
DCVC-FM	74.18	76.91	79.63	83.06	82.25	85.68
VCS	72.44	76.44	79.89	83.73	82.24	86.21
SMC	74.50	78.70	78.98	82.93	81.40	85.38
SMC++	75.48	80.12	80.55	84.91	82.43	86.43
Original	87.70	91.33	87.70	91.33	87.70	91.33

ing precise localization and robust feature extraction under occlusions. Results are shown in Table 2. At low bitrates like 0.01bpp, our SMC model outperforms FVC, PLVC, and VVC by 26.50%, 2.97%, and 5.98% in MOTA, respectively, matching DCVC-FM. Our SMC++ surpasses DCVC-FM by a large margin of 1.66%. Compared to the semantic coding approach VCS, SMC and SMC++ show a 3.05% and 4.72% MOTA gain, respectively.

At higher bitrates like 0.02bpp, DCVC-FM demonstrates strong performances, probably due to its internal high-resolution feature designs. Despite this, SMC++ closely matches DCVC-FM in MOTA (75.33% vs. 75.58%) and exceeds it in IDF1 (76.90% vs. 75.56%).

We also notice that, although FVC performs much better than the legacy HEVC codec on the action recognition task, it performs surprisingly poor on the MOT task, with a significantly lower MOTA (44.24% v.s. 61.30% of HEVC) at the 0.01bpp. This is due to FVC’s reliance on the hand-crafted

BPG codec for I frames and a neural codec for P frames, causing appearance inconsistency and hindering tracking consistency. DCVC-FM mitigates this through end-to-end optimization of I- and P-frame compression networks.

Finally, we provide the RP curves. As shown in the third row of Figure 4, SMC outperforms all previous methods except DCVC-FM, while SMC++ leads across most metrics. At higher bitrates, SMC++’s MOTP performance is unsatisfactory, which denotes the bounding-box accuracy of the detected objects. We conjecture the reasons is that the Transformer-based Blue-Tr module within SMC++ emphasizes high-level features and compromises local positioning accuracy. We plan to fix this by adaptively choosing between CNN- and Transformer-based compression modules.

Video Object Segmentation (VOS). We further evaluate different coding methods on the VOS task. As shown in Table 3, our basic SMC model surpasses all previous approaches, except VCS and DCVC-FM. For example, SMC exceeds VVC and PLVC by 6.73% and 12.75% in terms of $\mathcal{J}\&\mathcal{F}$ at the 0.01bpp level. After introducing the masked motion prediction and Blue-Tr module, our resultant SMC++ model outperforms VCS by 3.04% and 3.68% in terms of $\mathcal{J}\&\mathcal{F}$ and \mathcal{F} respectively, and DCVC-FM by 1.30% and 3.21% in the same metrics, at 0.01bpp. The RP curves of recent approaches are provided in the fourth row of Figure 4.

More Advanced Test Conditions. Recent learnable codecs [4] [140] [48] have adopted a more challenging test condition, *i.e.*, group-of-picture (GOP) size of 32. This larger GOP size poses a greater challenge than small GOP sizes, because of the error propagation issue. As shown in Figure 5, our advanced SMC++ model maintains its effectiveness under this more advanced test condition.

In the context of action recognition, SMC++ achieves approximately 2%, 5%, and 2% higher Top-1 accuracy compared to VVC, DCVC-FM, and VCS, respectively, on the HMDB51-SlowFast setting at 02bpp. Likewise, in the VOS task, SMC++ outperforms VVC, DCVC-FM, and VCS by about 5%, 2% and 2.2% in terms of the $\mathcal{J}\&\mathcal{F}$ metric, respectively, on the DAVIS2017-XMem setting at 0.01bpp.

Furthermore, it’s worth noting that the basic SMC model performs significantly worse than the VVC codec on the VOS task, despite being built upon and intended to enhance the VVC codec. For instance, at 0.01bpp, the VVC codec attains a $\mathcal{J}\&\mathcal{F}$ score of approximately 75%, whereas SMC manages only 70%. This discrepancy arises from SMC’s simple abstraction-based compression module, which struggles to handle the feature domain shift encountered in

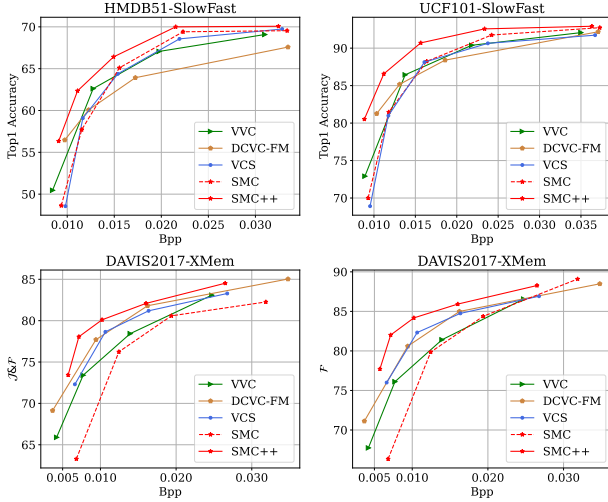


Fig. 5: Semantic coding performance of different methods on Action Recognition (1st row) and VOS (2nd row) tasks, evaluated on LDP mode with GOP size 32. The plot titles are in {Dataset}-{Task Model} format.

large GOP scenarios. In contrast, the SMC++ model boosts VVC’s performance by 5% $\mathcal{J}\&\mathcal{F}$ at 0.01bpp. This proves the Blueprint-based feature alignment operations in SMC++ effectively mitigates the error propagation problem.

Visual Quality Assessment. As shown in Table 4, our models SMC and SMC++ substantially outperform the previous traditional VVC, neural codec DCVC-FM, as well as semantic coding approach VCS in terms of perceptual visual quality, as evidenced by the much lower LPIPS values. We further demonstrate the frames compressed by different approaches. As shown in Figure 6, our approach shows sharper edges and better object structures than VVC and DCVC-FM, while showing fewer artifacts than VCS.

TABLE 4: Comparison of different methods on HEVC Class C. The results are reports in PSNR/LPIPS format. A lower LPIPS value indicates better perceptual quality.

	0.01bpp	0.02bpp	0.03bpp
VVC	24.32/0.4824	26.21/0.4104	27.46/0.3690
DCVC-FM	25.02/0.4927	27.11/0.4170	28.26/0.3778
VCS	20.86/0.5365	23.33/0.4062	23.81/0.3683
SMC	20.96/0.4083	23.29/0.3307	23.98/0.3058
SMC++	20.92/ 0.3936	23.92/ 0.3129	24.75/ 0.2890

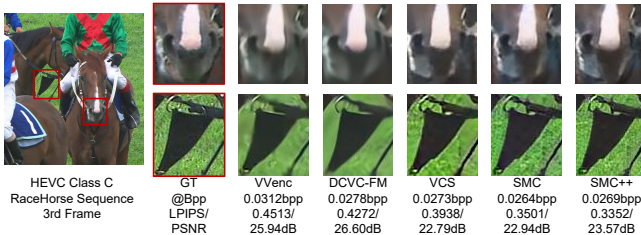


Fig. 6: Qualitative comparison of different approaches.

Towards High-fidelity Compression. Despite offering superior visual pleasure in perceptual quality, our approach yields lower PSNR results compared to VVC and DCVC-FM. For instance, as shown in Table 4, our SMC++ model lags behind DCVC-FM by roughly 3.5dB at the 0.03bpp level. Given the importance of high-fidelity decoding for the

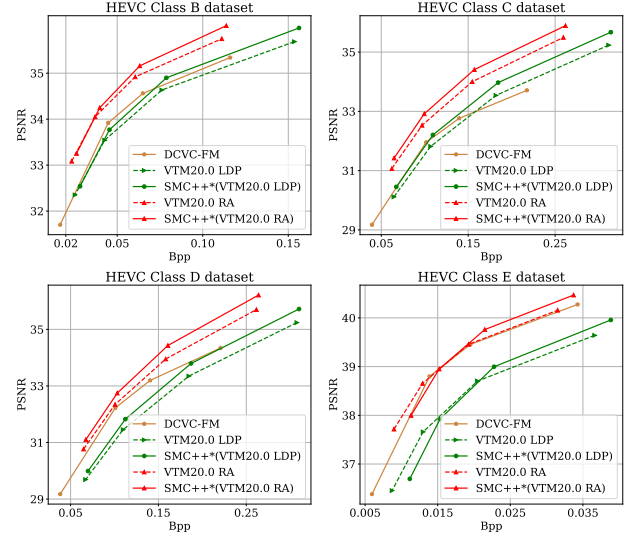


Fig. 7: Comparison of different coding methods in terms of PSNR. The test condition is 96 frames with intra-period 32. LDP and RA denote the Low-Delay P frame and Random Access mode, respectively.

secondary manual review of AI analysis results, we’ve enhanced our SMC++ model by appending a DR-Net, creating the SMC++* model. This aims to merge our decoded video with the lossy VVC-based video, enriching it with details. To match the performance of the state-of-the-art neural codec DCVC-FM [38], we utilize the advanced VTM20.0 software [39] as the base VVC coding layer. Since high-fidelity decoding usually requires a higher bitrate than semantic coding applications, we set the QP of the VTM20.0 software to larger values, *i.e.*, 23, 26, 29, and 32.

As shown in the green curves of Figure 7, when setting VTM20.0 to LDP mode, SMC++* notably improves performance on various datasets. For instance, on the HEVC class D dataset, we observe about 0.4dB PSNR gain at the 0.2bpp bitrate level. We also appended DR-Net to VCS and SMC models, training it for both, resulting in VCS* and SMC* models. On the HEVC class D dataset at the 0.2bpp bitrate level, VCS*, SMC*, and SMC++* achieved performances of 33.90dB, 33.82dB, and 34.01dB, respectively. This trend aligns with their semantic modeling capability, since good semantics is beneficial to video detail reconstruction [141].

Furthermore, when applied to the more advanced random access (RA) mode of VTM20.0, our SMC++* still demonstrates substantial improvements. As indicated by the red curves of Figure 7, we observe about 0.3dB quality enhancement at the 0.25bpp bitrate, on the HEVC class C dataset. We have observed that our method doesn’t enhance coding performance on the HEVC Class E dataset at low bitrates. This is likely because this dataset consists of conference videos with simplistic scenes and objects (humans and desks), lacking complex semantic elements like intricate object arrangements and interactions. As a result, the rich semantics learned by our approach aren’t particularly helpful in reconstructing these videos.

It seems like our non-semantic suppressed (NSS) learning strategy, excluding the non-semantic detail information from the coding procedure, is contradictory to the detail

decoding task. However, our framework indeed improves the base coding layer VTM, since this prompts a “divide-and-conquer” paradigm, where the VTM layer and our semantic layer focus on coding textual information and semantic information, respectively. The semantic information such as scene structure and object shape effectively corrects the distorted textures of VTM.

4.4 Ablation Studies and Analysis for SMC Model

Component Study. We first train a variant model denoted by *SMC wo Comp*, in which the semantic compensation operation is removed. As shown in Figure 8 (Left), the performance is drastically decreased by 16% in terms of Top1 accuracy at 0.02bpp. Further, we replace the simple UNet-Style visual-semantic fusion network of *SMC wo Comp* with a compressed video enhancement method *BasicVSR++* [142] [143]. The framework is degraded to a “lossy compression plus enhancement” paradigm. The improvement over the simple UNet is marginal and is still far behind our full semantic compensation framework by -14.23%@0.02bpp. These results prove that the distorted semantics cannot be fixed by video enhancement approaches and should be particularly compensated.

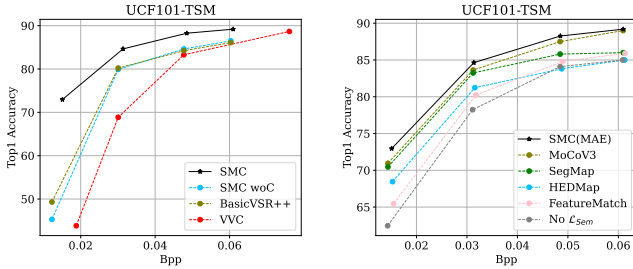


Fig. 8: *Left*: Ablation study on SMC framework. *SMC woC* denotes the semantic compensation procedure is removed. *BasicVSR++* denotes the compressed videos by VVC codec are enhanced by state-of-the-art BasicVSR++ method [142]. *Right*: Comparison of different semantic learning objectives.

TABLE 5: Impact of fine-tuning (FT) downstream model to different coding methods on UCF101-TSM (Top1) evaluation setting at the 0.04bpp bitrate level.

	VVC	VVC+BasicVSR++	SMC
Before FT(%)	76.97	82.46	86.46
After FT(%)	82.35(+5.38)	82.92(+0.46)	89.83(+3.37)

We also fine-tune the official UCF101-TSM model using videos compressed by the above variant methods. As shown in Table 5, the performance of vanilla VVC after fine-tuning (FT) nearly catches up with that of BasicVSR++ (82.46%), suggesting that the video enhancement procedure mainly narrows the domain gap between the evaluation and training video data input to TSM model, and bring no new information. In contrast, our full SMC framework further improves the accuracy from 86.46% (already higher than BasicVSR++) to 89.83% at 0.04bpp level. This proves that our method consistently benefits the downstream task by compensating new semantic information, whether fine-tuning the downstream model or not.

Different Semantic Learning Objectives \mathcal{L}_{Sem} . In this section, we train several SMC models by equipping

them with different learning objectives, *i.e.*, MoCoV3 [89], SegMap, HEDMap, and FeatureMatch. The first one is purely self-supervised. The latter three ones regularize the compressed video to be similar to the original video in terms of DeepLabv3 [144] semantic segmentation map, HED [145] edge map, and VGG16 [146] feature map, respectively.

TABLE 6: Impact of different self-supervised learning objectives to SMC performance, on action recognition and MOT tasks. Our masked learning paradigm performs much better, especially at the fine-grained MOT task.

UCF101-TSM@0.02bpp	MOT17-ByteTrack@0.01bpp
MoCoV3 → Masked Learning	MoCoV3 → Masked Learning
Top1: 75.20% → 76.48%	MOTA: 67.62% → 70.84%(+3.22%)

As shown in Table 6, our MAE-powered approach consistently outperforms the contrastive learning-based method MoCoV3 on two tasks of different granularities, *i.e.*, action recognition and MOT, by 1.28% Top1 accuracy and 3.22% MOTA, respectively. This clearly proves the semantics learned by MAE is more generalizable than that learned by contrastive learning, as well as more fine-grained.

We also demonstrate the superiority of the MAE learning objective over other heuristic objectives through experiments. A similar comparison has been conducted in our prior work [37]. We replicate this analysis for the sake of self-containment and to underscore that a similar conclusion applies to simpler network architectures of SMC model.

First, we find that the hand-crafted SegMap loss achieves similar performance to MoCoV3 in the lower bitrate ranges. However, this paradigm is still far behind our learning objective, *e.g.*, about a 3% performance gap at 0.05bpp level. After replacing the segmentation map with the HED edge map, the performance is further dropped, because the edge map does not contain the category information of each object region and is of less semantics. The model trained with FeatureMatch shows the worst results, probably because feature values are denser than the discretized segmentation/edge maps, which increases the bitcost.

Analysis on Masked Learning Objective. We first analyze the correlation between the masked learning loss \mathcal{L}_{MAE} and the semantic fidelity of the compressed video, which is defined as,

$$\text{Sem-FID}(\hat{X}) = -\log_{10}(\cos(\mathcal{F}(X), \mathcal{F}(\hat{X}))), \quad (7)$$

where \mathcal{F} denotes the video feature extractor network, \cos denotes the cosine distance, *i.e.*, $\cos(\mathbf{a}, \mathbf{b}) = 1 - \frac{\mathbf{a} \cdot \mathbf{b}}{\|\mathbf{a}\| \cdot \|\mathbf{b}\|}$. The larger Sem-FID value, the better the semantic similarity of the compressed video to the original video. As shown in Figure 9, the masked learning objective \mathcal{L}_{MAE} consistently serves as an effective semantic learning proxy for different downstream models such as TSM and TimeSformer.

Additionally, we visualize the videos reconstructed from the masked compressed videos under different bitrate levels. As shown in Figure 10, with more bitcost (0.0168bpp→0.0189bpp), the masked learning loss \mathcal{L}_{MAE} is reduced (0.0727→0.0703), resulting in better semantic fidelity, as quantified by larger *Sem - FID* metric (1.078→1.339). Despite a marginal reduction in \mathcal{L}_{MAE} , there is a remarkable enhancement in the semantic completeness, as evident in the areas marked by the red arrows. The analyses

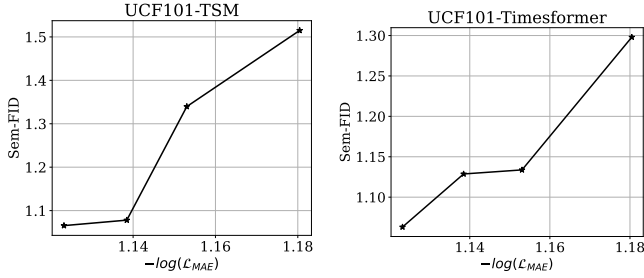


Fig. 9: Correlation analysis between \mathcal{L}_{MAE} and semantic fidelity of the reconstructed videos by SMC.

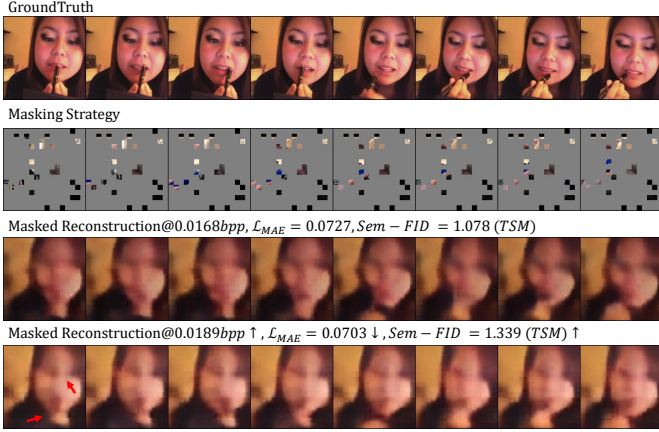


Fig. 10: Visualization of the MAE reconstructed videos at various bitrate levels. A lower MAE loss (4th row) leads to improved semantic appearance, particularly in the eyes and mouth regions, compared to a higher loss (3rd row).

TABLE 7: Impact of different masking ratios to SMC performance, on the UCF101-TSM setting at 0.02bpp.

Masking ratio	50%	75%	90%	95%
Top1(%)	73.85	75.62	76.48	76.08

TABLE 8: Comparison of different non-semantic suppression (NSS) strategies on UCF101-TSM setting. *Res* (bpp) denotes the bitcost of the residual semantic stream of SMC. The QP of the base codec VVC is set to 51.

	SMC VQ	SMC woSem	SMC woNSS	SMC
<i>Res</i> (bpp)	0.0048	0.0042	0.0074	0.0028
Top1 (%)	71.22	71.38	69.57	72.96

above consistently prove that the masked learning objective \mathcal{L}_{MAE} is a good surrogate objective for facilitating the compressed video to maintain the semantic information.

Further, we study the influence of the masking ratio on the semantic compression performance. As shown in Table 7, the 90% masking ratio achieves the optimal performance, and setting the masking ratio to 75% and 95% achieves slightly inferior performances. The 50% masking ratio shows a remarkable performance drop, as the textures can be simply completed by extending local textures, instead of reasoning high-level scene and structure semantics.

Effectiveness of NSS Strategy. Our method adapts the vanilla MAE to the semantic compression task by suppressing the non-semantic information within its token space.

To study the necessity of this design, we first train a variant model *SMC woNSS* by removing the \mathcal{L}_{NSS} item from

the loss function. As shown in Table 8, the bitcost of *SMC woNSS* is $2.6\times$ larger than the full SMC model, because the low-level pixel information is back-propagated to the coding system without any selection. Moreover, this non-semantic information may be noises to the downstream tasks, *i.e.*, the action recognition accuracy is dropped from 72.96% to 69.57%. Then, we train a variant model *SMC woSem* by using a plain learnable variable as the condition of the GMM distribution, instead of the semantic feature S . Both the compression efficiency and the recognition accuracy of *SMC woSem* are superior to *SMC woNSS*, but still inferior to our SMC model. This implies that explicitly regularizing the information entropy of the MAE token space is beneficial to a coding system, and using learned semantics as the guidance further improves this idea. Finally, we use the vector quantization (VQ) [147] codebook to discretize the token space of MAE, and the resultant *SMC VQ* model has similar performance to *SMC woSem*, indicating that the idea of information suppression is important for a compression system, instead of its concrete implementation.

Hyper-parameter Sensitivity. Setting the semantic loss item weight α to the values in the range [1,10] gives similar results. Setting the NSS loss item weight β to 0.1 achieve the best results, while a smaller value of 0.01 cannot effectively suppress the non-semantic information and a larger value of 1 makes the semantic learning item hard to optimize. Setting the GMM component number K to values in the range [3,9] gives similar results, while smaller K is slightly worse.

Bit-allocation Analysis. As shown in Figure 11, the semantic stream is always of high compression efficiency. Moreover, the bit allocation strategy is adaptive to the QP of the lossy visual stream, although we do not introduce any explicit adaptive design and time-consuming online rate-distortion optimization (RDO) strategies like [148]. The proportion of semantic information has been decreased to about 1% when QP is larger than 40 (the second column). This 1% bitcost boots Top1 accuracy by 7% on UCF101-TSM.

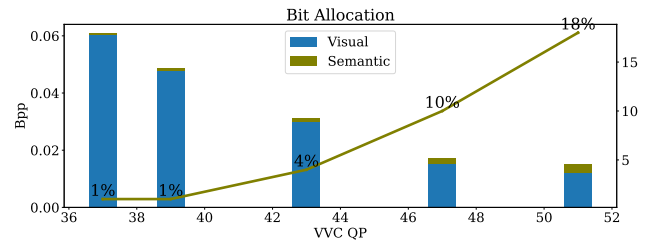


Fig. 11: Bit consumption of visual and residual semantic information in the SMC model. The x-axis indicates the QP value of the base-layer VVC codec in SMC.

Visualization of the Learned Semantics. As shown in Figure 12, the semantic feature extracted from the input frame is of high semantics and close to human perception. The activated regions are concentrated on the human body and the saliency objects, *i.e.*, vehicle wheels and drum. We further visualize the bitcost map of the residual part, where the redundant part is removed by subtracting the semantics in the lossy video stream. The residual bitcost map is quite sparse, and further concentrated on the AI task-interested regions. We also compare the VVC codec and our method in terms of qualitative results. As shown in (e)

and (f) of Figure 12, our method based on VVC (QP=51) demonstrates much clearer object structures and sharper edges than vanilla VVC (QP=47), while consuming few bits (0.08bpp *v.s.* 0.095bpp).

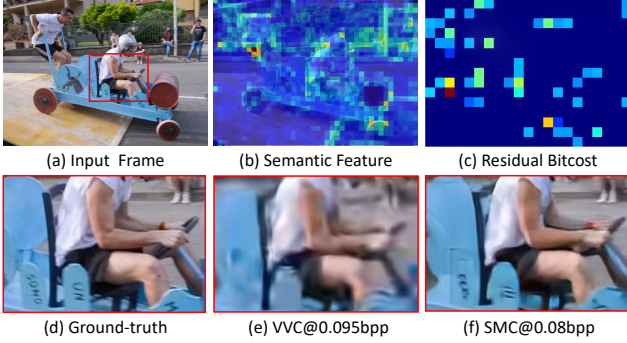


Fig. 12: Visualization of the semantic feature and the bitmap of the residual semantics within SMC. The red box region is zoomed in for more clearer visual comparison.

4.5 Analysis on the Improved SMC++ Model

In this section, we conduct comprehensive experiments to study the effectiveness of the newly added components in the SMC++ model, specifically: (1) the masked motion learning objective and (2) the Blueprint-guided compression Transformer (Blue-Tr). Considering that the SMC++ model requires more training iterations than the vanilla SMC model, we have accordingly increased the training iterations for the SMC model as well. This adjustment gives rise to the SMC^{adv} model, which serves as a more fair baseline.

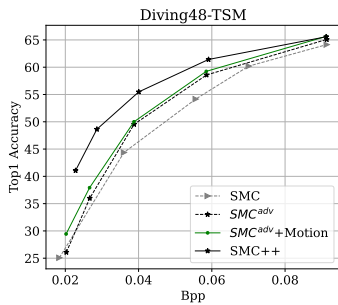


Fig. 13: Ablation study on the SMC++ framework: (1) SMC^{adv} shares the same details as the original SMC, but with extended training iterations to align with SMC++ for a fair comparison. (2) The SMC^{adv} +Motion model is trained with both masked appearance and motion modeling objectives. (3) The SMC++ model further improves SMC^{adv} +Motion model with Blue-Tr.

Effectiveness of the New Components. As shown in Figure 13, we train different variant models and evaluate them on the Diving48-TSM setting. First, we observe that by merely increasing the training iterations, neither changing the learning objective nor any network architecture, the resultant SMC^{adv} model has noticeably outperformed the original SMC model in our previous conference paper [36]. For instance, we note a substantial improvement of approximately 2% in performance at bitrate levels of 0.04bpp and 0.06bpp. Then, after introducing the masked motion learning objective, the resultant SMC^{adv} +Motion model achieves

a 3.2% Top1 accuracy advantage over the SMC^{adv} baseline, at the 0.02bpp level. This is because the additional motion target enhances the temporal modeling capability of our approach, allowing it to better discern video instances with ambiguous actions. Finally, the incorporation of our new Blue-Tr module leads to a notable enhancement, *i.e.*, the resultant SMC++ model (SMC^{adv} +Motion+Blue-Tr) achieves approximately 9% Top1 accuracy gain at the 0.03bpp bitrate level, when compared with the SMC^{adv} +Motion model. This proves that the specially designed Blue-Tr is powerful at compressing semantic information.

Different Masked Motion Prediction Objectives. Furthermore, we analyze the influence of different masked motion learning targets. We train three SMC variant models using three common motion representations as prediction targets, *i.e.*, RGB difference map, optical flow, and feature correlation map. RGB difference map is calculated by pixel-wise subtraction between each two consecutive frames. The optical flow is obtained with the pre-trained RAFT model [149]. As for the calculation of the feature correlation map, we first extract the feature map of video frames with the ResNet18 network, then calculate the correlation map [150] between the features of two consecutive frames. Compared to the optical flow map, the correlation map has a coarser resolution, but depicts more semantics.

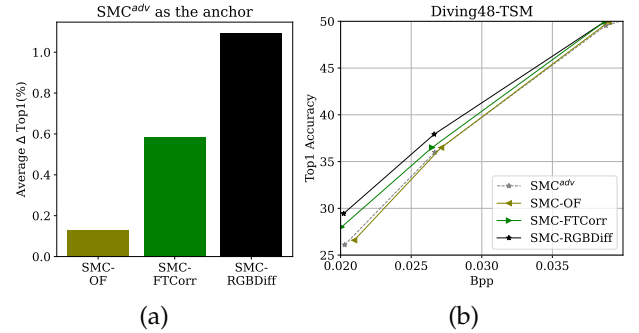


Fig. 14: Comparison of different masked motion targets.

As shown in Figure 14 (a), introducing motion prediction branch to the MAE learning objective always leads to the performance improvement. Compared to the computationally expensive feature-level matching operations in computing optical flow and correlation map, obtaining RGB difference map is more efficient. However, it demonstrates the strongest result, over 1% average Top1 accuracy improvement over the baseline SMC^{adv} model, obviously superior to the gains 0.15% and 0.6% that are obtained by optical flow and feature correlation. This is not surprising, as using frame difference as motion representation has effectively enhanced various video analysis tasks [151] [84] [152].

We further inspect the impact of different motion targets at various bit-rate levels, as shown in Figure 14 (b). At lower bitrate levels such as 0.02bpp, the performance gain of RGB difference is amplified as over 3% Top1 accuracy. In contrast, the performance gain of adopting the correlation map is inferior, *i.e.*, about 2% Top1 accuracy. When adopting the optical flow map, the performance is even hurt at low bitrates. We conjecture the reason is that predicting the complex optical flow is non-trivial for the lightweight decoder in the MAE framework, thus impeding the learning procedure. At higher bitrate levels (e.g., 0.04bpp), the gains of all motion-

enhanced models diminish, as appearance-based semantics are sufficiently discriminative.

Ablation Study on Blue-Tr. As shown in Figure 15 (a), all variant modules of Blue-Tr outperform the CNN-based basic compression module Basic-CM. This proves the advantage of Transformer over CNN in compressing highly abstract semantic information.

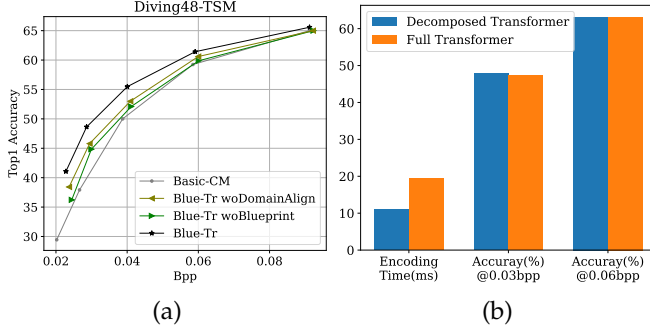


Fig. 15: (a) Ablation study of the proposed Blueprint-guide compression Transformer (Blue-Tr). “woBlueprint” denotes the blueprint-based alignment design is removed. “woDomainAlign” represents the domain alignment operation in Feature Aligner is excluded, and only the motion alignment is preserved. All models are trained with both masked-appearance and masked-motion modeling objectives for a fair comparison. (b) Comparison of the adopted decomposed Transformer and the vanilla full Transformer.

Furthermore, we note that removing the blueprint-based alignment, the resultant Blue-Tr woBlueprint model depicts a notable decrease in Top1 accuracy, *i.e.*, about 5% drop at a 0.04bpp bitrate. The reason is that, without explicit feature alignment, the Transformer still struggles to capture redundancies among various contextual features.

Moreover, to assess the impact of domain correction and motion compensation, we removed the Domain-Net from the Feature Aligner. The resulting model, Blue-Tr woDomainAlign, performs obviously worse than the full Blue-Tr, particularly at low bitrates. For instance, at 0.025bpp, there’s a performance dip of over 3%. This decline is attributed to the domain gap between the features of the lossy video (compressed by the base VVC codec) and our semantic features, which is further exacerbated by the severe semantic distortion of VVC in low-bitrate conditions.

We also investigate the effectiveness of the decomposed Transformer used in Blue-Tr. Specifically, a point-wise Transformer first removes redundancy among feature types, followed by a spatial Transformer to eliminate spatial redundancy. Figure 15 (b) demonstrates that our decomposition strategy enhances speed by about 2x compared to the standard Transformer (10.9ms vs. 20.2ms), while performance remains similar. Notably, our method slightly outperforms the standard Transformer at lower bitrate levels, achieving 47.75% vs. 47.23% at 0.03bpp, potentially because decomposition mitigate the feature ambiguity.

TABLE 9: Comparison of different Blueprint feature dimensions on the Diving48-TSM setting at 0.04bpp bitrate level.

Dimension	32	64	128	256	512
Top1 (%)	53.11	54.02	54.58	54.26	54.13

Finally, we explore how the blueprint semantic feature’s dimension impacts system performance. As shown in Table 9, smaller dimensions of 32 and 64 yield poorer results due to insufficient information for effective feature alignment. Conversely, larger dimensions like 256 and 512, while not causing drastic performance declines, still lead to a noticeable drop. This is because the bitcost savings from blueprint guidance can’t offset the cost of transmitting the blueprint feature itself.

4.6 Model Complexity and Running Time

As Table 10 demonstrates, our basic SMC model includes fewer parameters than the recent learnable codec DCVC-FM, but more parameters than the previous semantic coding approach VCS. VCS utilizes complex dynamic convolution in its encoder to enhance feature representation, striking a balance between parameter count and performance, albeit at the expense of a longer encoding time (1023ms vs. SMC’s 952ms). Furthermore, in the VCS, the semantic extraction and compression modules are tightly decoupled within the encoder network. In contrast, our SMC model separately employs a simple standard Resnet18 for semantic extraction, while isolating the semantic compression process into a distinct module. SMC’s simplicity and modular design make it a flexible and easily-extendable baseline.

TABLE 10: Model complexity and running time of different approaches. [†] denotes the method adopting the VVEnC software as the base coding layer, where the coding time consumed by VVEnC is incorporated. All evaluations are performed on a machine equipped with a single Nvidia 2080Ti GPU and Intel(R) Xeon(R) Silver 4116 CPU @ 2.10GHz. The running time was determined by encoding/decoding 100 frames of 1080p resolution and subsequently calculating the average time required for a single frame.

Method	Parameters	Encoding Time	Decoding time
VVEnC15.0	-	652ms	142ms
DCVC-FM	59.63M	833ms	654ms
VCS [†]	28.60M	1023ms	198ms
SMC [†]	48.23M	952ms	235ms
SMC++ [†]	96.18M	977ms	253ms

Our SMC++ model further introduces Transformer blocks, increasing the parameter count compared to SMC. However, the execution times are not obviously affected. This is because the new compression module Blue-Tr in SMC++, operating on significantly downsampled feature maps (32×), is extremely efficient.

5 CONCLUSION, LIMITATION, AND FUTURE WORK

In this paper, we have focused on a novel unsupervised video semantic compression problem. We have proposed a simple baseline model SMC to better cope with this problem, which is equipped with a novel non-semantics suppressed MAE loss. We have also proposed an advanced model SMC++, which improves SMC from two aspects, (1) a masked-motion learning objective and (2) a Transformer-based compression module. Comprehensive experiments demonstrate our method achieves remarkable results on three video analysis tasks with seven datasets.

One limitation is the learned semantics still rely on the training dataset consisting of natural images, which may not perform well in the professional field, such as medical image analysis. In the future, we plan to address this by devising the fast domain adaptation strategy. Moreover, motivated by the powerful semantics contained in large multi-modality models, we will attempt to transfer their rich semantic representation to our video semantic compression problem.

REFERENCES

- [1] G. J. Sullivan, J.-R. Ohm, W.-J. Han, and T. Wiegand, "Overview of the high efficiency video coding (hevc) standard," *TCSVT*, 2012.
- [2] B. Bross, Y.-K. Wang, Y. Ye, S. Liu, J. Chen, G. J. Sullivan, and J.-R. Ohm, "Overview of the versatile video coding (vvc) standard and its applications," *TCSVT*, 2021.
- [3] Z. Hu, G. Lu, and D. Xu, "Fvc: A new framework towards deep video compression in feature space," in *CVPR*, 2021.
- [4] J. Li, B. Li, and Y. Lu, "Deep contextual video compression," in *NeurIPS*, 2021.
- [5] C. Yi, S. Yang, H. Li, Y.-p. Tan, and A. Kot, "Benchmarking the robustness of spatial-temporal models against corruptions," in *NeurIPS*, 2021.
- [6] T. Tanaka, A. Harell, and I. V. Bajić, "Does video compression impact tracking accuracy?" in *ISCAS*, 2022.
- [7] X. Zhang, S. Ma, S. Wang, X. Zhang, H. Sun, and W. Gao, "A joint compression scheme of video feature descriptors and visual content," *TIP*, 2016.
- [8] J. Chao and E. Steinbach, "Keypoint encoding for improved feature extraction from compressed video at low bitrates," *TMM*, 2015.
- [9] L. Baroffio, M. Cesana, A. Redondi, M. Tagliasacchi, and S. Tubaro, "Hybrid coding of visual content and local image features," in *ICIP*, 2015.
- [10] L.-Y. Duan, Y. Lou, Y. Bai, T. Huang, W. Gao, V. Chandrasekhar, J. Lin, S. Wang, and A. C. Kot, "Compact descriptors for video analysis: The emerging mpeg standard," *TMM*, 2018.
- [11] L.-Y. Duan, V. Chandrasekhar, J. Chen, J. Lin, Z. Wang, T. Huang, B. Girod, and W. Gao, "Overview of the mpeg-cdvs standard," *TIP*, 2015.
- [12] L.-Y. Duan, F. Gao, J. Chen, J. Lin, and T. Huang, "Compact descriptors for mobile visual search and mpeg cdvs standardization," in *ISCAS*, 2013.
- [13] M. Makar, H. Lakshman, V. Chandrasekhar, and B. Girod, "Gradient preserving quantization," in *ICIP*, 2012.
- [14] L. Galteri, M. Bertini, L. Seidenari, and A. Del Bimbo, "Video compression for object detection algorithms," in *ICPR*, 2018.
- [15] H. Choi and I. V. Bajić, "High efficiency compression for object detection," in *ICASSP*, 2018.
- [16] H. Choi and I. V. Bajić, "Near-lossless deep feature compression for collaborative intelligence," in *MMSP*, 2018.
- [17] Z. Chen, K. Fan, S. Wang, L.-Y. Duan, W. Lin, and A. Kot, "Lossy intermediate deep learning feature compression and evaluation," in *ACM MM*, 2019.
- [18] Z. Chen, K. Fan, S. Wang, L. Duan, W. Lin, and A. C. Kot, "Toward intelligent sensing: Intermediate deep feature compression," *TIP*, 2019.
- [19] S. Singh, S. Abu-El-Hajja, N. Johnston, J. Ballé, A. Shrivastava, and G. Toderici, "End-to-end learning of compressible features," in *ICIP*, 2020.
- [20] R. Feng, X. Jin, Z. Guo, R. Feng, Y. Gao, T. He, Z. Zhang, S. Sun, and Z. Chen, "Image coding for machines with omnipotent feature learning," *ECCV*, 2022.
- [21] X. Sheng, L. Li, D. Liu, and H. Li, "Vnvc: A versatile neural video coding framework for efficient human-machine vision," *TPAMI*, 2024.
- [22] K. Liu, D. Liu, L. Li, N. Yan, and H. Li, "Semantics-to-signal scalable image compression with learned reversible representations," *IJCV*, 2021.
- [23] S. Yang, Y. Hu, W. Yang, L.-Y. Duan, and J. Liu, "Towards coding for human and machine vision: Scalable face image coding," *TMM*, 2021.
- [24] N. Yan, C. Gao, D. Liu, H. Li, L. Li, and F. Wu, "Sssic: Semantics-to-signal scalable image coding with learned structural representations," *TIP*, 2021.
- [25] H. Choi and I. V. Bajić, "Latent-space scalability for multi-task collaborative intelligence," in *ICIP*, 2021.
- [26] H. Choi and I. V. Bajić, "Scalable image coding for humans and machines," *TIP*, 2022.
- [27] S. Sun, T. He, and Z. Chen, "Semantic structured image coding framework for multiple intelligent applications," *TCSVT*, 2020.
- [28] H. Lin, B. Chen, Z. Zhang, J. Lin, X. Wang, and T. Zhao, "Deepsvic: Deep scalable video coding for both machine and human vision," in *ACM MM*, 2023.
- [29] V. Bhaskaran and K. Konstantinides, "Image and video compression standards: algorithms and architectures," 1997.
- [30] Z. Wang, A. C. Bovik, H. R. Sheikh, and E. P. Simoncelli, "Image quality assessment: from error visibility to structural similarity," *TIP*, 2004.
- [31] K. He, X. Chen, S. Xie, Y. Li, P. Dollár, and R. Girshick, "Masked autoencoders are scalable vision learners," in *CVPR*, 2022.
- [32] Z. Tong, Y. Song, J. Wang, and L. Wang, "Videomae: Masked autoencoders are data-efficient learners for self-supervised video pre-training," *NeurIPS*, 2022.
- [33] X. Dong, J. Bao, T. Zhang, D. Chen, W. Zhang, L. Yuan, D. Chen, F. Wen, and N. Yu, "Bootstrapped masked autoencoders for vision bert pretraining," in *ECCV*, 2022.
- [34] K. Simonyan and A. Zisserman, "Two-stream convolutional networks for action recognition in videos," in *NeurIPS*, 2014.
- [35] A. Vaswani, N. Shazeer, N. Parmar, J. Uszkoreit, L. Jones, A. N. Gomez, Ł. Kaiser, and I. Polosukhin, "Attention is all you need," in *NeurIPS*, 2017.
- [36] Y. Tian, G. Lu, G. Zhai, and Z. Gao, "Non-semantics suppressed mask learning for unsupervised video semantic compression," in *ICCV*, 2023.
- [37] Y. Tian, G. Lu, Y. Yan, G. Zhai, L. Chen, and Z. Gao, "A coding framework and benchmark towards low-bitrate video understanding," *TPAMI*, 2024.
- [38] J. Li, B. Li, and Y. Lu, "Neural video compression with feature modulation," in *CVPR*, 2024.
- [39] "Vtm-20.0," https://vcgit.hhi.fraunhofer.de/jvet/VVCSoftware_VTM/-/releases/VTM-20.0, 2023.
- [40] T. Wiegand, G. J. Sullivan, G. Bjontegaard, and A. Luthra, "Overview of the h. 264/avc video coding standard," *TCSVT*, 2003.
- [41] F. Zhang and D. R. Bull, "A parametric framework for video compression using region-based texture models," *JSTSP*, 2011.
- [42] G. Lu, X. Zhang, W. Ouyang, L. Chen, Z. Gao, and D. Xu, "An end-to-end learning framework for video compression," *TPAMI*, 2020.
- [43] D. Ma, F. Zhang, and D. R. Bull, "Bvi-dvc: A training database for deep video compression," *TMM*, 2021.
- [44] Z. Chen, G. Lu, Z. Hu, S. Liu, W. Jiang, and D. Xu, "Lsvc: A learning-based stereo video compression framework," in *CVPR*, 2022.
- [45] G. Lu, T. Zhong, J. Geng, Q. Hu, and D. Xu, "Learning based multi-modality image and video compression," in *CVPR*, 2022.
- [46] G. Lu, W. Ouyang, D. Xu, X. Zhang, C. Cai, and Z. Gao, "Dvc: An end-to-end deep video compression framework," in *CVPR*, 2019.
- [47] J. Li, B. Li, and Y. Lu, "Hybrid spatial-temporal entropy modelling for neural video compression," in *ACM MM*, 2022.
- [48] Li, Jiahao and Li, Bin and Lu, Yan, "Neural video compression with diverse contexts," in *CVPR*, 2023.
- [49] Y. Tian, G. Lu, X. Min, Z. Che, G. Zhai, G. Guo, and Z. Gao, "Self-conditioned probabilistic learning of video rescaling," in *ICCV*, 2021.
- [50] Y. Tian, Y. Yan, G. Zhai, L. Chen, and Z. Gao, "Clsa: a contrastive learning framework with selective aggregation for video rescaling," *TIP*, 2023.
- [51] F. Zhang, C. Feng, and D. R. Bull, "Enhancing vvc through cnn-based post-processing," in *ICME*, 2020.
- [52] Z. Wang, E. P. Simoncelli, and A. C. Bovik, "Multiscale structural similarity for image quality assessment," in *ACSSC*, 2003.
- [53] R. Yang, L. Van Gool, and R. Timofte, "Perceptual learned video compression with recurrent conditional gan," *IJCAI*, 2022.
- [54] F. Mentzer, E. Agustsson, J. Ballé, D. Minnen, N. Johnston, and G. Toderici, "Neural video compression using gans for detail synthesis and propagation," in *ECCV*, 2022.

- [55] Z. Huang, C. Jia, S. Wang, and S. Ma, "Visual analysis motivated rate-distortion model for image coding," in *ICME*, 2021.
- [56] J. Choi and B. Han, "Task-aware quantization network for jpeg image compression," in *ECCV*, 2020.
- [57] Q. Cai, Z. Chen, D. O. Wu, S. Liu, and X. Li, "A novel video coding strategy in hevc for object detection," *TCSVT*, 2021.
- [58] Q. Zhang, S. Wang, X. Zhang, S. Ma, and W. Gao, "Just recognizable distortion for machine vision oriented image and video coding," *IJCV*, 2021.
- [59] A. I. Veselov, H. Chen, F. Romano, Z. Zhijie, and M. R. Gilmudtinov, "Hybrid video and feature coding and decoding," 2021.
- [60] N. Le, H. Zhang, F. Cricri, R. Ghaznavi-Youvalari, and E. Rahtu, "Image coding for machines: an end-to-end learned approach," in *ICASSP*, 2021.
- [61] Y. Bai, X. Yang, X. Liu, J. Jiang, Y. Wang, X. Ji, and W. Gao, "Towards end-to-end image compression and analysis with transformers," in *AAAI*, 2022.
- [62] Z. Yang, Y. Wang, C. Xu, P. Du, C. Xu, C. Xu, and Q. Tian, "Discernible image compression," in *ACMMM*, 2020.
- [63] L. Duan, J. Liu, W. Yang, T. Huang, and W. Gao, "Video coding for machines: A paradigm of collaborative compression and intelligent analytics," *TIP*, 2020.
- [64] Y. Hu, S. Yang, W. Yang, L.-Y. Duan, and J. Liu, "Towards coding for human and machine vision: A scalable image coding approach," in *ICME*, 2020.
- [65] S. Duan, H. Chen, and J. Gu, "Jpd-se: High-level semantics for joint perception-distortion enhancement in image compression," *TIP*, 2022.
- [66] Y. Dubois, B. Bloem-Reddy, K. Ullrich, and C. J. Maddison, "Lossy compression for lossless prediction," in *NeurIPS*, 2021.
- [67] K. He, H. Fan, Y. Wu, S. Xie, and R. Girshick, "Momentum contrast for unsupervised visual representation learning," in *CVPR*, 2020.
- [68] M. Akbari, J. Liang, and J. Han, "Dsslic: Deep semantic segmentation-based layered image compression," in *ICASSP*, 2019.
- [69] D. Huang, X. Tao, F. Gao, and J. Lu, "Deep learning-based image semantic coding for semantic communications," in *GLOBECOM*, 2021.
- [70] C. Zhu, G. Lu, R. Xie, and L. Song, "Perceptual video coding based on semantic-guided texture detection and synthesis," in *PCS*, 2022.
- [71] J. Chang, Q. Mao, Z. Zhao, S. Wang, S. Wang, H. Zhu, and S. Ma, "Layered conceptual image compression via deep semantic synthesis," in *ICIP*, 2019.
- [72] J. Chang, Z. Zhao, C. Jia, S. Wang, L. Yang, Q. Mao, J. Zhang, and S. Ma, "Conceptual compression via deep structure and texture synthesis," *TIP*, 2022.
- [73] J. Chang, Z. Zhao, L. Yang, C. Jia, J. Zhang, and S. Ma, "Thousand to one: Semantic prior modeling for conceptual coding," in *ICME*, 2021.
- [74] J. Chang, J. Zhang, Y. Xu, J. Li, S. Ma, and W. Gao, "Consistency-contrast learning for conceptual coding," in *ACMMM*, 2022.
- [75] Q. Liu, B. Liu, Y. Wu, W. Li, and N. Yu, "Real-time online multi-object tracking in compressed domain," *arXiv*, 2022.
- [76] S. Wang, H. Lu, and Z. Deng, "Fast object detection in compressed video," in *ICCV*, 2019.
- [77] C. Li, X. Wang, L. Wen, D. Hong, T. Luo, and L. Zhang, "End-to-end compressed video representation learning for generic event boundary detection," in *CVPR*, 2022.
- [78] X. Wang, Z. Huang, B. Liao, L. Huang, Y. Gong, and C. Huang, "Real-time and accurate object detection in compressed video by long short-term feature aggregation," *CVIU*, 2021.
- [79] B. Zhang, L. Wang, Z. Wang, Y. Qiao, and H. Wang, "Real-time action recognition with enhanced motion vector cnns," in *CVPR*, 2016.
- [80] Z. Zheng, L. Yang, Y. Wang, M. Zhang, L. He, G. Huang, and F. Li, "Dynamic spatial focus for efficient compressed video action recognition," *TCSVT*, 2023.
- [81] C.-Y. Wu, M. Zaheer, H. Hu, R. Manmatha, A. J. Smola, and P. Krähenbühl, "Compressed video action recognition," in *CVPR*, 2018.
- [82] Z. Shou, X. Lin, Y. Kalantidis, L. Sevilla-Lara, M. Rohrbach, S.-F. Chang, and Z. Yan, "Dmc-net: Generating discriminative motion cues for fast compressed video action recognition," in *CVPR*, 2019.
- [83] J. Carreira and A. Zisserman, "Quo vadis, action recognition? a new model and the kinetics dataset," in *CVPR*, 2017.
- [84] Y. Tian, Y. Yan, G. Zhai, G. Guo, and Z. Gao, "Ean: event adaptive network for enhanced action recognition," *IJCV*, 2022.
- [85] Y. Tian, Z. Che, W. Bao, G. Zhai, and Z. Gao, "Self-supervised motion representation via scattering local motion cues," in *ECCV*, 2020.
- [86] Y. Tian, X. Min, G. Zhai, and Z. Gao, "Video-based early and detection via temporal pyramid networks," in *ICME*, 2019.
- [87] S. H. Khatoonabadi and I. V. Bajic, "Video object tracking in the compressed domain using spatio-temporal markov random fields," *TIP*, 2012.
- [88] A. S. Khattak, N. Anjum, N. Khan, M. R. Mufti, and N. Ramzan, "Amf-mspf: A retrospective analysis with online object tracking algorithms," *Displays*, 2022.
- [89] X. Chen, H. Fan, R. Girshick, and K. He, "Improved baselines with momentum contrastive learning," *arXiv*, 2020.
- [90] T. Chen, S. Kornblith, M. Norouzi, and G. Hinton, "A simple framework for contrastive learning of visual representations," in *ICML*, 2020.
- [91] T. Pan, Y. Song, T. Yang, W. Jiang, and W. Liu, "Videomoco: Contrastive video representation learning with temporally adversarial examples," in *CVPR*, 2021.
- [92] J. Zhou, C. Wei, H. Wang, W. Shen, C. Xie, A. Yuille, and T. Kong, "ibot: Image bert pre-training with online tokenizer," *ICLR*, 2022.
- [93] Y. Tian, C. Sun, B. Poole, D. Krishnan, C. Schmid, and P. Isola, "What makes for good views for contrastive learning?" in *NeurIPS*, 2020.
- [94] H. Bao, L. Dong, S. Piao, and F. Wei, "Beit: Bert pre-training of image transformers," in *ICLR*, 2022.
- [95] X. Chen, M. Ding, X. Wang, Y. Xin, S. Mo, Y. Wang, S. Han, P. Luo, G. Zeng, and J. Wang, "Context autoencoder for self-supervised representation learning," *IJCV*, 2024.
- [96] Z. Xie, Z. Zhang, Y. Cao, Y. Lin, J. Bao, Z. Yao, Q. Dai, and H. Hu, "Simim: A simple framework for masked image modeling," in *CVPR*, 2022.
- [97] X. Dong, J. Bao, T. Zhang, D. Chen, W. Zhang, L. Yuan, D. Chen, F. Wen, and N. Yu, "Peco: Perceptual codebook for bert pre-training of vision transformers," in *AAAI*, 2023.
- [98] C. Wei, H. Fan, S. Xie, C.-Y. Wu, A. Yuille, and C. Feichtenhofer, "Masked feature prediction for self-supervised visual pre-training," in *CVPR*, 2022.
- [99] Y. Song, M. Yang, W. Wu, D. He, F. Li, and J. Wang, "It takes two: Masked appearance-motion modeling for self-supervised video transformer pre-training," *arXiv*, 2022.
- [100] X. Sun, P. Chen, L. Chen, C. Li, T. H. Li, M. Tan, and C. Gan, "Masked motion encoding for self-supervised video representation learning," in *CVPR*, 2023.
- [101] K. He, X. Zhang, S. Ren, and J. Sun, "Deep residual learning for image recognition," in *CVPR*, 2016.
- [102] O. Ronneberger, P. Fischer, and T. Brox, "U-net: Convolutional networks for biomedical image segmentation," in *MICCAI*, 2015.
- [103] D. A. Reynolds *et al.*, "Gaussian mixture models." *Encyclopedia of biometrics*, 2009.
- [104] A. Papoulis and S. Unnikrishna Pillai, *Probability, random variables and stochastic processes*, 2002.
- [105] J. Ballé, D. Minnen, S. Singh, S. J. Hwang, and N. Johnston, "Variational image compression with a scale hyperprior," *ICLR*, 2018.
- [106] Z. Cheng, H. Sun, M. Takeuchi, and J. Katto, "Learned image compression with discretized gaussian mixture likelihoods and attention modules," in *CVPR*, 2020.
- [107] J. A. Hartigan and M. A. Wong, "Algorithm as 136: A k-means clustering algorithm," *Journal of the Royal Statistical Society. Series C*, 1979.
- [108] L. Van der Maaten and G. Hinton, "Visualizing data using t-sne." *JMLR*, 2008.
- [109] X. Chen and K. He, "Exploring simple siamese representation learning," in *CVPR*, 2021.
- [110] P. Esser, R. Rombach, and B. Ommer, "Taming transformers for high-resolution image synthesis," in *CVPR*, 2021.
- [111] R. Zhang, P. Isola, A. A. Efros, E. Shechtman, and O. Wang, "The unreasonable effectiveness of deep features as a perceptual metric," in *CVPR*, 2018.
- [112] J. Ballé, V. Laparra, and E. P. Simoncelli, "End-to-end optimized image compression," *ICLR*, 2017.

- [113] Y. Hu, W. Yang, and J. Liu, "Coarse-to-fine hyper-prior modeling for learned image compression," in *AAAI*, 2020.
- [114] Z. Hu, G. Lu, J. Guo, S. Liu, W. Jiang, and D. Xu, "Coarse-to-fine deep video coding with hyperprior-guided mode prediction," in *CVPR*, 2022.
- [115] L. Chen, H. Zhang, J. Xiao, L. Nie, J. Shao, W. Liu, and T.-S. Chua, "Sca-cnn: Spatial and channel-wise attention in convolutional networks for image captioning," in *CVPR*, 2017.
- [116] J. Dai, H. Qi, Y. Xiong, Y. Li, G. Zhang, H. Hu, and Y. Wei, "Deformable convolutional networks," in *ICCV*, 2017.
- [117] B. Xu, N. Wang, T. Chen, and M. Li, "Empirical evaluation of rectified activations in convolutional network," *arXiv*, 2015.
- [118] F. Mentzer, G. D. Toderici, D. Minnen, S. Caelles, S. J. Hwang, M. Lucic, and E. Agustsson, "Vct: A video compression transformer," in *NeurIPS*, 2022.
- [119] K. Soomro, A. R. Zamir, and M. Shah, "Ucf101: A dataset of 101 human actions classes from videos in the wild," *arXiv*, 2012.
- [120] H. Kuehne, H. Jhuang, E. Garrote, T. Poggio, and T. Serre, "Hmdb: a large video database for human motion recognition," in *ICCV*, 2011.
- [121] Y. Li, Y. Li, and N. Vasconcelos, "Resound: Towards action recognition without representation bias," in *ECCV*, 2018.
- [122] A. Milan, L. Leal-Taixé, I. Reid, S. Roth, and K. Schindler, "Mot16: A benchmark for multi-object tracking," *arXiv*, 2016.
- [123] J. Pont-Tuset, F. Perazzi, S. Caelles, P. Arbeláez, A. Sorkine-Hornung, and L. Van Gool, "The 2017 davis challenge on video object segmentation," *arXiv*, 2017.
- [124] J. Lin, C. Gan, and S. Han, "Tsm: temporal shift module for efficient video understanding," in *ICCV*, 2019.
- [125] C. Feichtenhofer, H. Fan, J. Malik, and K. He, "Slowfast networks for video recognition," in *ICCV*, 2019.
- [126] G. Bertasius, H. Wang, and L. Torresani, "Is space-time attention all you need for video understanding?" *ICML*, 2021.
- [127] "Openmmlab's next generation video understanding toolbox and benchmark," <https://github.com/open-mmlab/mmdetection2>, 2020.
- [128] Y. Zhang, P. Sun, Y. Jiang, D. Yu, Z. Yuan, P. Luo, W. Liu, and X. Wang, "Bytetrack: Multi-object tracking by associating every detection box," *ECCV*, 2022.
- [129] "Mmtracking: Openmmlab video perception toolbox and benchmark," <https://github.com/open-mmlab/mmdetection2>, 2020.
- [130] H. K. Cheng and A. G. Schwing, "Xmem: Long-term video object segmentation with an atkinson-shiffrin memory model," *ECCV*, 2022.
- [131] S. Tomar, "Converting video formats with ffmpeg," *Linux Journal*, 2006.
- [132] A. Wiecekowsky, J. Brandenburg, T. Hinz, C. Bartnik, V. George, G. Hege, C. Helmrich, A. Henkel, C. Lehmann, C. Stoffers, I. Zupancic, B. Bross, and D. Marpe, "Vvenc: An open and optimized vvc encoder implementation," in *ICMEW*.
- [133] R. Kasturi, D. Goldgof, P. Soundararajan, V. Manohar, J. Garofolo, R. Bowers, M. Boonstra, V. Korzhova, and J. Zhang, "Framework for performance evaluation of face, text, and vehicle detection and tracking in video: Data, metrics, and protocol," *TPAMI*, 2008.
- [134] A. Dosovitskiy, L. Beyer, A. Kolesnikov, D. Weissenborn, X. Zhai, T. Unterthiner, M. Dehghani, M. Minderer, G. Heigold, S. Gelly *et al.*, "An image is worth 16x16 words: Transformers for image recognition at scale," in *ICLR*, 2021.
- [135] Y. Li, B. Ji, X. Shi, J. Zhang, B. Kang, and L. Wang, "Tea: Temporal excitation and aggregation for action recognition," in *CVPR*, 2020.
- [136] S. Bai, J. Z. Kolter, and V. Koltun, "An empirical evaluation of generic convolutional and recurrent networks for sequence modeling," *arXiv*, 2018.
- [137] D. P. Kingma and J. Ba, "Adam: A method for stochastic optimization," *ICLR*, 2014.
- [138] A. Paszke, S. Gross, F. Massa, A. Lerer, J. Bradbury, G. Chanan, T. Killeen, Z. Lin, N. Gimeshein, L. Antiga *et al.*, "Pytorch: An imperative style, high-performance deep learning library," in *NeurIPS*, 2019.
- [139] "Ecm-12.0," <https://vcgit.hhi.fraunhofer.de/ecm/ECM/-/tags/ECM-12.0>, 2023.
- [140] Y.-H. Ho, C.-P. Chang, P.-Y. Chen, A. Gnutti, and W.-H. Peng, "Canf-vc: Conditional augmented normalizing flows for video compression," in *ECCV*, 2022.
- [141] Z. Lu, Z. Xiao, J. Bai, Z. Xiong, and X. Wang, "Can sam boost video super-resolution?" *arXiv*, 2023.
- [142] K. C. Chan, S. Zhou, X. Xu, and C. C. Loy, "Basicvsr++: Improving video super-resolution with enhanced propagation and alignment," in *CVPR*, 2022.
- [143] Chan, Kelvin CK and Zhou, Shangchen and Xu, Xiangyu and Loy, Chen Change, "On the generalization of basicvsr++ to video deblurring and denoising," *arXiv*, 2022.
- [144] L.-C. Chen, G. Papandreou, F. Schroff, and H. Adam, "Rethinking atrous convolution for semantic image segmentation," *arXiv*, 2017.
- [145] S. Xie and Z. Tu, "Holistically-nested edge detection," in *ICCV*, 2015.
- [146] K. Simonyan and A. Zisserman, "Very deep convolutional networks for large-scale image recognition," *arXiv*, 2014.
- [147] A. Van Den Oord, O. Vinyals *et al.*, "Neural discrete representation learning," in *NeurIPS*, 2017.
- [148] G. Lu, C. Cai, X. Zhang, L. Chen, W. Ouyang, D. Xu, and Z. Gao, "Content adaptive and error propagation aware deep video compression," in *ECCV*, 2020.
- [149] Z. Teed and J. Deng, "Raft: Recurrent all-pairs field transforms for optical flow," in *ECCV*, 2020.
- [150] A. Dosovitskiy, P. Fischer, E. Ilg, P. Hausser, C. Hazirbas, V. Golkov, P. Van Der Smagt, D. Cremers, and T. Brox, "FlowNet: Learning optical flow with convolutional networks," in *ICCV*, 2015.
- [151] L. Wang, Z. Tong, B. Ji, and G. Wu, "Tdn: Temporal difference networks for efficient action recognition," in *CVPR*, 2021.
- [152] Y. Liu, Z. Tu, L. Lin, X. Xie, and Q. Qin, "Real-time spatio-temporal action localization via learning motion representation," in *ACCVW*, 2020.